

Global Stability Analysis of a Fractional-Order Ebola Epidemic Model with Control Strategies

1

2

3

4

Abstract

5

6

7

8

9

10

11

12

13

14

15

16

17

18

19

We proposed a fractional-order derivative model for Ebola virus disease (EVD) to assess the effects of control strategies on the spread of the disease in the population. The proposed model incorporates all relevant biological factors, health education campaigns, prevention measures, and treatment as control strategies. We computed the basic reproduction number \mathcal{R}_0 and qualitatively used it to assess the existence of the model states. In particular, we noted that two equilibrium points exist, the disease-free and endemic equilibrium points which are both globally stable whenever $\mathcal{R}_0 < 1$ and $\mathcal{R}_0 > 1$ respectively. We performed sensitivity analysis on the key parameters that drive the EVD dynamics to determine their relative importance in EVD transmission and prevalence. Model parameters were estimated using the 2014 Ebola outbreak in Guinea. Further, numerical simulation results are presented using fractional Adam-Bashforth-Moulton scheme to support the analytical findings. From the numerical simulations, we have noted that as α decreases from unit, the solution profiles of the model attain its stability much faster than at $\alpha = 1$. Furthermore, the results demonstrated that the aforementioned control strategies have the potential to reduce the transmission of EVD in the population.

20

21

Keywords: Lyapunov; Control Strategies; Ebola model; Fractional-order derivatives; Model stability; Data fitting; Model validation.

22 1 Introduction

23 Ebola virus disease (EVD) is a disease caused by Ebola virus in humans and other non-human
24 primates like gorillas, chimpanzees and duikers. The virus originated in fruit bats and jumped
25 to humans through animals such as chimpanzees [1, 2]. The disease first appeared in 1976 in
26 two outbreaks, one in Sudan and the other in Democratic Republic of Congo (DRC). Since
27 then, the disease has continued to appear in Africa several times, for example, in Ivory Coast
28 and Gabon in 1994; in Uganda in 2000; in Guinea in 2014; and again in DRC in 2019.

29 The EVD outbreaks, particularly in Western part of Africa, continue to present substantial
30 challenges to health and health-care resources in the region and beyond. According to the
31 World Health organization (WHO), more than 11000 people died in the region between 2013
32 and 2016 due to the outbreak of EVD [3]. In particular, Sierra Leone alone recorded more
33 than 14,100 Ebola cases which resulted in over 3900 deaths, and more than 30000 individuals
34 were quarantined due to possible Ebola exposure [4].

35 Although several factors such as poor health facilities and highly populated urban areas
36 have been attributed to perpetuate EVD during an outbreak, funeral and burial practices
37 anchored in certain traditional and religious practices of the West African communities are
38 regarded as one of the leading factors that fuel the spread of EVD in the region [5, 6]. As most
39 communities in West Africa believe in life after death, funeral and burial practices are given a
40 lot of significance and perceived as crucial steps in transitioning from the world of the living
41 to the spiritual world [7]. Individuals from this region believe that the transition should be
42 facilitated by surviving relatives through funeral and burial rituals. Communities perceive that
43 if the deceased does not attain the elevated rank of ancestral spirit, their spirit may return
44 and punish the living relatives [6]. Hence, several unique funeral and burial practices that
45 more often involve excessive contact with a corpse are often performed to appease the dead. In
46 its global alert and response report of WHO concurred with this assertion by suggesting that
47 nearly 60% of all Ebola cases in Guinea between 2013 and 2014 were a result of traditional
48 burial practices [8]. Cognizant of this, it is essential to gain a better and more comprehensive
49 understanding of the impact of funeral and burial practices during EVD outbreaks to develop
50 feasible intervention and management strategies. Among the several tools and techniques that
51 can be used to explore this phenomenon is mathematical modeling.

52 Mathematical modelling, as a powerful tool in quantifying the complex and numerous
53 factors, has been widely developed to explore the transmission of EVD [9, 10, 11]. Mathematical

54 modeling is described as the conversion of a real problem in a mathematical form. Modeling,
55 therefore, involves the formulation of the real-life situations or converting the problems in
56 mathematical explanations to a real or believable situation (see for example [12, 13].

57 Mathematical models with classical-order differential equations have especially received
58 great attention (see, [14, 15, 16, 17, 18]) and have widely been used in disease modeling.
59 However, recent studies suggest that models with integer-order derivatives do not adequately
60 capture hereditary properties, long-range interactions, and memory effects that exist in biolog-
61 ical systems which have many applications in the fields of science, compared to fractional-order
62 derivatives [19, 20, 21, 22, 23]. It is documented literature that models that utilize fractional-
63 order derivatives capture hereditary properties, memory effects, and enlarge the region of
64 stability [23]. Previous studies suggest that without memory effects evolution and control
65 of diseases in communities can not be considered [24]. In particular, whenever the disease
66 spreads in societies, humans gain experience which influence in control of spread disease in the
67 community [23, 25]. Additionally, cell membrane of living organisms contain some fractional
68 order-electrical conductance which are classified in groups of fractional order models [19, 24].

69 Recently, Ivan et al. [26], Muhammad et al. [27], Dokuyucua and Dutta [28], Farman et
70 al.[29], Singh[30] and Pan et al. [31] used the fractional-order derivatives to study the effect
71 of memory on EVD dynamics. Dokuyucua and Dutta [28] utilised Caputo fractional-order
72 differential equations without singular kernel to explore the effects of memory on spread of
73 Ebola in Africa. Among several other outcomes, they found out that their model solution-
74 s were in agreement with reality. Muhammad et al. [27] proposed and studied a nonlinear
75 time-fractional mathematical model of the Ebola Virus to understand the outbreak of dis-
76 ease in the community. Their model analysis included both Caputo and Atangana Baleanu
77 fractional derivative operators to solve the solution of the system of fractional differential e-
78 quations. One of the key findings from their work was that fractional-order derivative showed
79 significant changes and memory effects compared to classical-order derivatives. Farman et
80 al. [29] studied a nonlinear fractional order Ebola virus mathematical model to explore the
81 effects control strategies on the spread of disease in the population. They used Laplace with
82 Adomian Decomposition to solved the fractional differential systems. Their results revealed
83 that, as the order of derivative decreased, the disease died out in the population. Area et al.
84 [26] used both classical and fractional order Ebola epidemic model to fit the real data of Ebola
85 cases reported in Guinea, Liberia and Sierra Leone. In numerical simulations, they found that
86 the fractional-order model gave a better prediction of the disease compared to classical order

87 derivatives. Mathematical studies of fractional order differential equations in disease modeling
88 are also found in [24, 32, 33, 34, 35, 36, 37, 38] and the references therein.

89 Mathematical modelling, as a powerful tool in quantifying the complex and numerous
90 factors, has widely been developed to explore the transmission dynamics of EVD [9, 10, 11].
91 One of the emerging areas in biological research is to understand the role of memory effects on
92 the short and long-term dynamics of infectious diseases. Thus, in this study a mathematical
93 model for EVD based on Fractional Calculus is proposed and analyzed. Although this is not the
94 first study to incorporate Fractional Calculus in analyzing EVD transmission (see, for example
95 [26, 30, 39], the proposed model is unique from those in literature in that it also incorporates
96 the direct and indirect disease transmission rates, and effects of cultural beliefs and educational
97 campaigns on funeral and burial practices. Here, EVD transmission rate is being modeled by
98 the mass action incidence which is appropriate when the population is not too large [40]. One
99 of the most commonly performed funeral rituals, which significantly contributes to the spread
100 of Ebola, is the washing and cleaning of dead bodies. Another burial ritual involves relatives
101 of the deceased washing their hands in a common bowl after which they touch the face of
102 the deceased in what is perceived as a ‘love touch’ that cements unity between the living and
103 ancestral spirits [41]. We assume that the transmission rate of EVD is dependent on the size of
104 the population attending funerals and the burial practices which implies that the contact rate
105 is an increasing function of the population. The mass action incidence is density- dependent
106 since contact rate per infective is proportional to the density of infectious hosts.

107 Motivated by the above-mentioned works, we derive a fractional-order model for EVD
108 based on the Caputo derivative. The choice of Caputo derivative is also aided by the fact
109 that the Caputo derivative for a given function which is constant is zero. Thus, the Caputo
110 operator computes an ordinary differential equation, followed by a fractional integral to obtain
111 the desired order of fractional derivative [33, 42, 43]. Most importantly, the Caputo fractional
112 derivative allows the use of local initial conditions to be included in the derivation of the model
113 [25, 30, 43, 44].

114 In Section 2, we present the preliminaries on the Caputo fractional calculus. The proposed
115 model and analytical results are presented in Section 3. In Section 4, the numerical simulations
116 are done to verify the theoretical results presented in the study. Finally, a concluding remark
117 rounds up the paper.

118 2 Preliminary Results

119 The basic idea of fractional order derivative was first initiated by Riemann and Liouville, and
 120 another by Caputo which is based on the exponential kernel. The main advantage of Caputo
 121 fractional order derivative over Riemann-Liouville fractional operator is that: Caputo fractional
 122 order derivative provides standard initial conditions which have clear physical interpretation of
 123 the problem. Besides, Caputo fractional order derivative is bounded, meaning that the deriva-
 124 tive of any constant function is zero. Motivated by the benefits of Caputo fractional operator
 125 over the other operators, the proposed model in this study is based on the Caputo fractional
 126 derivatives which is an important tool for describing the memory and heredity properties.

127 2.1 Mathematical concepts of fractional order

128 In this section we start with mathematical concepts of of Caputo fractional order derivatives
 129 which will be used in analysis of proposed Ebola model (see,[24, 45]). The details can be
 130 obtained in Appendix A.

131 3 Description of Model and Analytical Results

132 Motivated by the works in [9, 10, 11, 26, 39, 30], we are concerned with the impact of ed-
 133 ucational campaigns on funeral and burial practices. We subdivide the total population of
 134 humans $N(t)$ into categories of: susceptible population unaware of the disease fighting means
 135 $S(t)$, susceptible population aware of the disease fighting means $E(t)$; infected individuals who
 136 are displaying clinical signs of the disease and are infectious $I(t)$, individuals who have recov-
 137 ered from infection $R(t)$, and the deceased population $D(t)$. Let $P(t)$ denote the pathogen
 138 population in the environment.

139 The EVD transmission rate is modeled by the mass action incidence which is appropriate
 140 when $N(t)$ is not too large [40]. We assume that the transmission rate is dependent on the
 141 size of the population which implies that the contact rate is an increasing function of the
 142 population. The mass action incidence is density- dependent since the contact rate per infective
 143 is proportional to the density of the infectious host.

144 The proposed fractional-order derivatives EVD model is given by:

145

$$\left. \begin{aligned}
 D_{t_0}^\alpha S(t) &= \Lambda - (\beta_1 I(t) + \beta_2 D(t) + \lambda P(t))S(t) + \phi E(t) - (\mu + \psi)S(t), \\
 D_{t_0}^\alpha E(t) &= \psi S(t) - \gamma(\beta_1 I(t) + \beta_2 D(t) + \lambda P(t))E(t) - (\phi + \mu)E(t), \\
 D_{t_0}^\alpha I(t) &= (\beta_1 I(t) + \beta_2 D(t) + \lambda P(t))(S(t) + \gamma E(t)) - (\mu + \sigma + \delta)I(t), \\
 D_{t_0}^\alpha R(t) &= \sigma I(t) - \mu R(t), \\
 D_{t_0}^\alpha D(t) &= (\mu + \delta)I(t) - \epsilon D(t), \\
 D_{t_0}^\alpha P(t) &= \rho I(t) + \theta D(t) - (\tau + \eta)P(t),
 \end{aligned} \right\} \quad (1)$$

147 where $D_{t_0}^\alpha$ denotes the Caputo-fractional calculus and α with $0 < \alpha \leq 1$ is the fractional order.

148 The model flow diagram is depicted in Figure 1.

149 Additional biological and epidemiological assumptions that govern the model (1) are::

150 (i) Model (1) exhibits some time dimension problems between left-and right-hand sides of
 151 the equations. On the left, the dimension is $(time)^{-\alpha}$, whereas on the right-hand side
 152 the dimension is $(time)^{-1}$. To balance the model, the corrected system corresponding to
 153 model (1) is as follows:

$$\left. \begin{aligned}
 D_{t_0}^\alpha S(t) &= \Lambda^\alpha - (\beta_1^\alpha I(t) + \beta_2^\alpha D(t) + \lambda^\alpha P(t))S(t) + \phi^\alpha E(t) - (\mu^\alpha + \psi^\alpha)S(t), \\
 D_{t_0}^\alpha E(t) &= \psi^\alpha S(t) - \gamma^\alpha(\beta_1^\alpha I(t) + \beta_2^\alpha D(t) + \lambda^\alpha P)E(t) - (\phi^\alpha + \mu^\alpha)E(t), \\
 D_{t_0}^\alpha I(t) &= (\beta_1^\alpha I(t) + \beta_2^\alpha D(t) + \lambda^\alpha P(t))(S(t) + \gamma^\alpha E(t)) - (\mu^\alpha + \sigma^\alpha + \delta^\alpha)I(t), \\
 D_{t_0}^\alpha R(t) &= \sigma^\alpha I(t) - \mu^\alpha R(t), \\
 D_{t_0}^\alpha D(t) &= (\mu^\alpha + \delta^\alpha)I(t) - \epsilon^\alpha D(t), \\
 D_{t_0}^\alpha P(t) &= \rho^\alpha I(t) + \theta^\alpha D(t) - (\tau^\alpha + \eta^\alpha)P(t),
 \end{aligned} \right\} \quad (2)$$

155 (ii) All new recruits are assumed to be susceptible and unaware of the disease and recruited
 156 at the rate Λ . Natural mortality occurs at the rate μ . Meanwhile, the susceptible
 157 populations are educated at the rate ψ per-day and some educated populations can stop
 158 following the preventive measures at the rate ϕ . There is evidence in [46, 47] that Ebola
 159 outbreak can last for more than two years which allows the demographic process to take
 160 place. Therefore, we have included vital dynamics in our model since the 2014 Ebola
 161 outbreak in Guinea.

162 (iii) Susceptible unaware individuals become aware of the infection through educational cam-
 163 paigns at the rate ψ . Due to memory fading and/or carelessness, susceptible aware
 164 individuals become unaware individuals at the rate ϕ :

- 165 (iv) Susceptible individuals are assumed to acquire the infection either directly (through con-
 166 tact with either infectious individuals or deceased EVD patients) or, indirectly through
 167 contaminated environment. Model parameters β_1, β_2 and λ account for disease transmis-
 168 sion when susceptible individuals come into contact with infectious individuals, deceased
 169 patients and the environment respectively. Susceptible aware individuals are assumed
 170 to have reduced chances of contracting the disease, modeled by $0 < \gamma < 1$, where γ is
 171 the disease modification factor that accounts for the impact of educational campaigns on
 172 disease transmission.
- 173 (v) Infected individuals either recover from infection permanently (at the rate σ) or, succumb
 174 to disease-related death at the rate δ . The deceased individual are buried after ϵ^{-1} days.
 175 Infectious and deceased EVD patients contaminate the environment at the rates ρ and θ ,
 176 respectively. The population of pathogens in the environment decreases due to natural
 177 decay (at the rate τ) or decontamination (at the rate η).

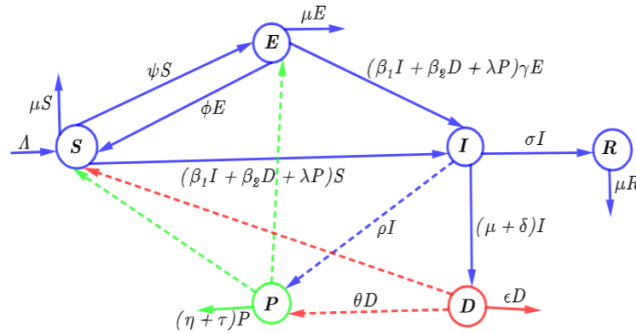


Figure 1: Flow chart for Ebola virus disease

178 3.1 Non-negativity and boundedness of model solutions

179 Since model (2) investigate human population, it is important to demonstrate that all model
 180 solutions are bounded and positive for all $t \geq 0$. From the computations presented in Appendix
 181 B we obtained the following results.

182 **Theorem 3.1.** *Model (2) has unique and non-negative solutions which turn into region Γ_+ as*

183 $t \rightarrow \infty$, where Γ_+ is defined by: $\Gamma_+ = \left\{ (S(t), E(t), I(t), R(t), D(t), P(t)) \in \mathbb{R}_+^6; S(t) + E(t) + \right.$
 184 $I(t) + R(t) + D(t) + P(t) = N = \frac{\Lambda^\alpha}{\mu^\alpha}, D = \frac{(\mu^\alpha + \delta^\alpha)\Lambda^\alpha}{\mu^\alpha \epsilon^\alpha}, P = \frac{\epsilon^\alpha \rho^\alpha \Lambda^\alpha + \theta^\alpha (\mu^\alpha + \delta^\alpha) \Lambda^\alpha}{\mu^\alpha \epsilon^\alpha (\tau^\alpha + \eta^\alpha)} \left. \right\}$

185 3.2 The Basic Reproduction Number

186 In this section, we study the basic reproduction number and the existence of a disease-free equi-
 187 librium and an endemic equilibrium of the model (2). The model (2) always has a disease-free
 188 equilibrium $\mathcal{E}^0 = (S^0, E^0, I^0, D^0, P^0, R^0) = (S^0, E^0, 0, 0, 0, 0)$, with $S^0 = \frac{\Lambda^\alpha(\phi^\alpha + \mu^\alpha)}{\mu^\alpha(\mu^\alpha + \phi^\alpha + \psi^\alpha)}$,
 189 $E^0 = \frac{\Lambda^\alpha\psi^\alpha}{\mu^\alpha(\mu^\alpha + \phi^\alpha + \psi^\alpha)}$, and $S^0 + \gamma^\alpha E^0 = \frac{\Lambda^\alpha(\phi^\alpha + \mu^\alpha + \gamma^\alpha\psi^\alpha)}{\mu^\alpha(\mu^\alpha + \phi^\alpha + \psi^\alpha)}$. By means of the next gen-
 190 eration matrix (see, for example, van den Driessche and Watmough [18], one obtains the basic
 191 reproduction number of the model (2) as follows:

$$\begin{aligned} \mathcal{R}_0 = & \frac{(S^0 + \gamma^\alpha E^0)\beta_1^\alpha}{(\mu^\alpha + \sigma^\alpha + \delta^\alpha)} + \frac{(S^0 + \gamma^\alpha E^0)(\mu^\alpha + \delta^\alpha)\beta_2^\alpha}{\epsilon^\alpha(\mu^\alpha + \sigma^\alpha + \delta^\alpha)} + \frac{(S^0 + \gamma^\alpha E^0)\theta^\alpha(\mu^\alpha + \delta^\alpha)\lambda^\alpha}{\epsilon^\alpha(\tau^\alpha + \eta^\alpha)(\mu^\alpha + \sigma^\alpha + \delta^\alpha)} \\ & + \frac{(S^0 + \gamma^\alpha E^0)\rho^\alpha\lambda^\alpha}{(\tau^\alpha + \eta^\alpha)(\mu^\alpha + \sigma^\alpha + \delta^\alpha)} \end{aligned} \quad (3)$$

193 Biologically, the basic reproduction number \mathcal{R}_0 represents the average number of new or
 194 secondary EVD infections caused by the introduction of an infectious individual into a to-
 195 tally susceptible population. It follows that model (2) has a disease-free equilibrium point
 196 $\mathcal{E}^0 = (S^0, E^0, I^0, D^0, P^0, R^0)$ which exists whenever $\mathcal{R}_0 < 1$ and it provides a criterion for the
 197 extinction of the disease. In addition to the disease-free equilibrium \mathcal{E}^0 , the model (2) has a
 198 unique endemic equilibrium point $\mathcal{E}^* = (S^*, E^*, I^*, D^*, P^*, R^*)$, which exists whenever $\mathcal{R}_0 > 1$,
 199 the EVD infection persists, where:

$$S^* = \frac{\Lambda^\alpha[\gamma^\alpha(\beta_1^\alpha I^* + \beta_2^\alpha D^* + \lambda^\alpha P^*) + (\mu^\alpha + \phi^\alpha)]}{n_1 n_2 - \phi^\alpha \psi^\alpha}, \quad (4)$$

$$E^* = \frac{\Lambda^\alpha \psi^\alpha}{n_1 n_2 - \phi^\alpha \psi^\alpha}, \quad (5)$$

203 with $n_1 = [(\beta_1^\alpha I^* + \beta_2^\alpha D^* + \lambda^\alpha P^*) + (\mu^\alpha + \psi^\alpha)]$ and $n_2 = [\gamma^\alpha(\beta_1^\alpha I^* + \beta_2^\alpha D^* + \lambda^\alpha P^*) + (\mu^\alpha + \phi^\alpha)]$

$$\begin{aligned} D^* = \frac{(\mu^\alpha + \delta^\alpha)I^*}{\epsilon^\alpha}, \quad R^* = \frac{\rho^\alpha I^*}{\mu^\alpha}, \quad \text{and} \\ P^* = \frac{\rho^\alpha I^*}{(\tau^\alpha + \eta^\alpha)} + \frac{\theta^\alpha(\mu^\alpha + \delta^\alpha)I^*}{\epsilon^\alpha(\tau^\alpha + \eta^\alpha)}. \end{aligned} \quad (6)$$

205 Substituting equation (6) into the third equation in (2), gives:

$$\begin{aligned} \beta_1^\alpha I^*(S^* + \gamma^\alpha E^*) + \frac{\beta_2^\alpha(\mu^\alpha + \delta^\alpha)I^*(S^* + \gamma^\alpha E^*)}{\epsilon^\alpha} + \frac{\lambda^\alpha \rho^\alpha I^*(S^* + \gamma^\alpha E^*)}{(\tau^\alpha + \eta^\alpha)} \\ + \frac{\lambda^\alpha \theta^\alpha(\mu^\alpha + \delta^\alpha)I^*(S^* + \gamma^\alpha E^*)}{\epsilon^\alpha(\tau^\alpha + \eta^\alpha)} - (\mu^\alpha + \sigma^\alpha + \delta^\alpha)I^* = 0. \end{aligned} \quad (7)$$

207 From (31), we have:

$$\begin{aligned}
 & \left(\frac{\beta_1^\alpha I^*(S^* + \gamma^\alpha E^*)}{(\mu^\alpha + \sigma^\alpha + \delta^\alpha)} + \frac{\beta_2^\alpha (\mu^\alpha + \delta^\alpha) I^*(S^* + \gamma^\alpha E^*)}{\epsilon^\alpha (\mu^\alpha + \sigma^\alpha + \delta^\alpha)} + \frac{\lambda^\alpha \rho^\alpha I^*(S^* + \gamma^\alpha E^*)}{(\tau^\alpha + \eta^\alpha) (\mu^\alpha + \sigma^\alpha + \delta^\alpha)} \right. \\
 & \left. + \frac{\lambda^\alpha \theta^\alpha (\mu^\alpha + \delta^\alpha) I^*(S^* + \gamma^\alpha E^*)}{\epsilon^\alpha (\tau^\alpha + \eta^\alpha) (\mu^\alpha + \sigma^\alpha + \delta^\alpha)} - 1 \right) \times (\mu^\alpha + \sigma^\alpha + \delta^\alpha) I^* = 0.
 \end{aligned}$$

209 It follows that:

$$I^* = 0, \quad \text{or}$$

$$(S^* + \gamma^\alpha E^*) = \frac{\epsilon^\alpha (\tau^\alpha + \eta^\alpha) (\mu^\alpha + \sigma^\alpha + \delta^\alpha)}{r}, \quad (8)$$

213 with $r = \beta_1^\alpha \epsilon^\alpha (\tau^\alpha + \eta^\alpha) + \beta_2^\alpha \eta^\alpha (\mu^\alpha + \delta^\alpha) + \lambda^\alpha \epsilon^\alpha \rho^\alpha + \theta^\alpha \lambda^\alpha (\mu^\alpha + \delta^\alpha)$. Substituting the value of
 214 S^* and E^* into (32), yields:

$$g(I^*) = A(I^*)^2 + BI^* + C, \quad (9)$$

216 where:

$$\begin{aligned}
 A &= \epsilon^\alpha (\tau^\alpha + \eta^\alpha) (\mu^\alpha + \sigma^\alpha + \delta^\alpha) \gamma^\alpha \lambda^{2\alpha} \times \left[\frac{\rho^\alpha}{(\tau^\alpha + \eta^\alpha)} + \frac{\theta^\alpha (\mu^\alpha + \delta^\alpha)}{\epsilon^\alpha (\tau^\alpha + \eta^\alpha)} \right]^2 \\
 &+ \epsilon^\alpha (\tau^\alpha + \eta^\alpha) (\mu^\alpha + \sigma^\alpha + \delta^\alpha) \gamma^\alpha \beta_1^{\alpha c} + \frac{(\tau^\alpha + \eta^\alpha) (\mu^\alpha + \sigma^\alpha + \delta^\alpha) \gamma^\alpha \beta_2^{2\alpha} (\mu^\alpha + \delta^\alpha)^2}{\epsilon^\alpha} \\
 &+ 2(\tau^\alpha + \eta^\alpha) (\mu^\alpha + \sigma^\alpha + \delta^\alpha) (\mu^\alpha + \delta^\alpha) \gamma^\alpha \beta_1^\alpha \beta_2^\alpha + 2\gamma^\alpha \beta_1^\alpha \lambda^\alpha (\mu^\alpha + \sigma^\alpha + \delta^\alpha) (\rho^\alpha \epsilon^\alpha + \theta^\alpha (\mu^\alpha \\
 &+ \delta^\alpha)) + 2\gamma^\alpha \beta_2^\alpha \lambda^\alpha (\mu^\alpha + \sigma^\alpha + \delta^\alpha) (\mu^\alpha + \delta^\alpha) \times \left(\rho^\alpha + \frac{\theta^\alpha (\mu^\alpha + \delta^\alpha)}{\epsilon^\alpha} \right), \\
 B &= \left[\gamma^\alpha \mu^\alpha + (\mu^\alpha + \phi^\alpha + \gamma^\alpha \psi^\alpha) - \frac{M}{\epsilon^\alpha (\tau^\alpha + \eta^\alpha) (\mu^\alpha + \sigma^\alpha + \delta^\alpha)} \right] \\
 &\times (\mu^\alpha + \sigma^\alpha + \delta^\alpha) [\beta_1^\alpha \epsilon^\alpha (\tau^\alpha + \eta^\alpha) + \beta_2^\alpha (\tau^\alpha + \eta^\alpha) (\mu^\alpha + \delta^\alpha) + \lambda^\alpha \epsilon^\alpha \rho^\alpha + \theta^\alpha \lambda^\alpha (\mu^\alpha + \delta^\alpha)], \\
 C &= \epsilon^\alpha \mu^\alpha (\tau^\alpha + \eta^\alpha) (\mu^\alpha + \sigma^\alpha + \delta^\alpha) (\mu^\alpha + \phi^\alpha + \psi^\alpha) [1 - \mathcal{R}_0], \text{ where,}
 \end{aligned}$$

$$217 \quad M = \gamma^\alpha \Lambda^\alpha (\beta_1^\alpha \epsilon^\alpha (\tau^\alpha + \eta^\alpha) + \beta_2^\alpha (\tau^\alpha + \eta^\alpha) (\mu^\alpha + \delta^\alpha) + \lambda^\alpha \epsilon^\alpha \rho^\alpha + \theta^\alpha \lambda^\alpha (\mu^\alpha + \delta^\alpha)).$$

218 Using the fact that all parameters in the model (2) are positive for $t \geq 0$, it follows from
 219 Equation (9) that $A > 0$. Furthermore, $C > 0$ when $\mathcal{R}_0 < 1$. Therefore, the number of

220 possible positive real roots of the polynomial (9) hinges on the signs of B and C . By applying
 221 the Descartes rule of signs on the polynomial (9) $g(I^*) = 0$, given in (9), we list the various
 222 possibilities for the roots of $g(I^*)$ in Table 1:

Table 1: Number of various possibilities for the roots of $g(I^*)$ for $\mathcal{R}_0 < 1$ and $\mathcal{R}_0 > 1$.

Case	A	B	C	\mathcal{R}_0	No. of sign changes	No. of various possibilities for the roots
1	+	+	+	$\mathcal{R}_0 < 1$	0	0
2	+	+	-	$\mathcal{R}_0 > 1$	1	1
3	+	-	+	$\mathcal{R}_0 < 1$	2	0,2
4	+	-	-	$\mathcal{R}_0 > 1$	1	1

223 Based on the various possibilities in Table 1, we have the following results:

224 **Theorem 3.2.** *The model (2) admits that:*

- 225 (i) *a unique endemic equilibrium \mathcal{E}^* if $\mathcal{R}_0 > 1$ and Cases 2 and 4 are satisfied,*
- 226 (ii) *more than one endemic equilibrium if $\mathcal{R}_0 < 1$ part of Case 3 holds,*
- 227 (iii) *no endemic equilibrium if $\mathcal{R}_0 < 1$, and Cases 1 and part of Case 3 are satisfied.*

228 3.3 Global Stability

229 In this section, we are concerned with the global stability of the disease-free equilibrium $\mathcal{E}^0 =$
 230 $(S^0, E^0, 0, 0, 0, 0)$ and the endemic equilibrium $\mathcal{E}^* = (S^*, E^*, I^*, D^*, P^*, R^*)$ of the model (2).
 231 To investigate the global stability of the model steady states we will construct appropriate
 232 Lyapunov functionals. Since the recovered/removed population does not contribute to the
 233 generation of secondary infections one can ignore that fourth equation of model (2) when
 234 examining the global stability and consider the following reduced system:

$$\left. \begin{aligned}
 D_{t_0}^\alpha S(t) &= \Lambda^\alpha - (\beta_1^\alpha I(t) + \beta_2^\alpha D(t) + \lambda^\alpha P(t))S(t) + \phi^\alpha E(t) - m_1 S(t), \\
 D_{t_0}^\alpha E(t) &= \psi^\alpha S(t) - \gamma^\alpha (\beta_1^\alpha I(t) + \beta_2^\alpha D(t) + \lambda^\alpha P)E(t) - m_2 E(t), \\
 D_{t_0}^\alpha I(t) &= [(\beta_1^\alpha I(t) + \beta_2^\alpha D(t) + \lambda^\alpha P(t))S(t) + \gamma^\alpha (\beta_1^\alpha I(t) + \beta_2^\alpha D(t) + \lambda^\alpha P)E(t)] \\
 &\quad - m_3 I(t), \\
 D_{t_0}^\alpha D(t) &= m_4 I(t) - \epsilon^\alpha D(t), \\
 D_{t_0}^\alpha P(t) &= \rho^\alpha I(t) + \theta^\alpha D(t) - m_5 P(t),
 \end{aligned} \right\} (10)$$

236 with $m_1 = (\mu^\alpha + \psi^\alpha)$, $m_2 = (\phi^\alpha + \mu^\alpha)$, $m_3 = (\mu^\alpha + \sigma^\alpha + \delta^\alpha)$, $m_4 = (\mu^\alpha + \delta^\alpha)$, and $m_5 = (\tau^\alpha + \eta^\alpha)$.
 237 To investigate the global stability of the disease-free equilibrium point \mathcal{E}^0 and the endemic
 238 equilibrium \mathcal{E}^* of model (10), we utilize the Lyapunov function whose origin is ecology but
 239 was extended to epidemiology models and then effectively applied to a variety of compartment
 240 models (see for example [52]).

241 We begin by introducing the following definition of positive definite function (see, [53]) that
 242 we use to develop the Lyapunov's function.

243 **Definition 1. (Positive definite function [53])** Let $\mathcal{V}(t) : \mathbb{R}^n \rightarrow \mathbb{R}$ be a continuously
 244 differentiable real valued function. Then $\mathcal{V}(t)$ is said to be positive definite function if:

- 245 1. $\mathcal{V}(t^0) = 0$, and:
- 246 2. $\mathcal{V}(t) > 0$ for all $t \neq t^0$

247 **Theorem 3.3.** (Fractional La-Salle invariance principle [24, 45]). Let $x^* \in \Gamma \subset \mathbb{R}^n$ be
 248 an equilibrium point for the non-autonomous fractional order system $D_{t_0}^\alpha = f(t, x)$. Let $L : [0, \infty) \times \Gamma \rightarrow \mathbb{R}$
 249 be a continuously differentiable function such that:

$$250 \quad \mathcal{M}_1(x) \leq L(t, x(t)) \leq \mathcal{M}_2(x)$$

251 and:

$$252 \quad D_{t_0}^\alpha L(t, x(t)) \leq -\mathcal{M}_3(x),$$

253 for all $\alpha \in (0, 1)$ and all $x \in \Gamma$, where $\mathcal{M}_1(x)$, $\mathcal{M}_2(x)$ and $\mathcal{M}_3(x)$ are continuous positive
 254 definite functions on Γ . Then the equilibrium point x^* is uniformly asymptotically stable.

255 Now using Theorem (3.3) we will show that the disease-free equilibrium \mathcal{E}^0 and the endemic
 256 equilibrium point \mathcal{E}^* of system (10) are globally asymptotically stable

257 **Theorem 3.4.** For $\alpha \in (0, 1]$, the disease-free equilibrium \mathcal{E}^0 of system (10) is globally asymp-
 258 totically stable whenever $\mathcal{R}_0 \leq 1$.

259 *Proof.* Consider the following appropriate Lyapunov function:

$$260 \quad \mathcal{V}(t) = \left(\frac{\beta_1^\alpha}{m_3} + \frac{\beta_2^\alpha m_4}{\epsilon^\alpha m_3} + \frac{\theta^\alpha \lambda^\alpha m_4}{\epsilon^\alpha m_5 m_3} + \frac{\lambda^\alpha \rho^\alpha}{m_5 m_3} \right) I(t) + \left(\frac{\beta_2^\alpha}{\epsilon^\alpha} + \frac{\theta^\alpha \lambda^\alpha}{\epsilon^\alpha m_5} \right) D(t) + \frac{\lambda^\alpha}{m_5} P(t).$$

261 Then the time fractional order derivative of $\mathcal{V}(t)$ along solutions of model (10):

$$D_{t_0}^\alpha \mathcal{V}(t) = \left(\frac{\beta_1^\alpha}{m_3} + \frac{\beta_2^\alpha m_4}{\epsilon^\alpha m_3} + \frac{\theta^\alpha \lambda^\alpha m_4}{\epsilon^\alpha m_5 m_3} + \frac{\lambda^\alpha \rho^\alpha}{m_5 m_3} \right) \times \left(\beta_1^\alpha I(t) + \beta_2^\alpha D(t) + \lambda^\alpha P(t) \right)$$

$$\begin{aligned}
 & \times \left(S(t) + \gamma^\alpha E(t) \right) - \left(\beta_1^\alpha I(t) + \beta_2^\alpha D(t) + \lambda^\alpha P(t) \right) \\
 & = \left[\left(\frac{\beta_1^\alpha}{m_3} + \frac{\beta_2^\alpha m_4}{\epsilon^\alpha m_3} + \frac{\theta^\alpha \lambda^\alpha m_4}{\epsilon^\alpha m_5 m_3} + \frac{\lambda^\alpha \rho^\alpha}{m_5 m_3} \right) \times \left(S(t) + \gamma^\alpha E(t) \right) - 1 \right] \\
 & \quad \times \left[\beta_1^\alpha I(t) + \beta_2^\alpha D(t) + \lambda^\alpha P(t) \right].
 \end{aligned}$$

262

263 Since $S^0 \leq S(t), E^0 \leq E(t), \left(S^0 + \gamma^\alpha E^0 = \frac{\Lambda^\alpha(\phi^\alpha + \mu^\alpha + \gamma^\alpha \psi^\alpha)}{\mu^\alpha(\mu^\alpha + \phi^\alpha + \psi^\alpha)} \right)$ for $t \geq 0$ we have:

$$\begin{aligned}
 D_{t_0}^\alpha \mathcal{V}(t) & \leq \left[\left(\frac{\beta_1^\alpha}{m_3} + \frac{\beta_2^\alpha m_4}{\epsilon^\alpha m_3} + \frac{\theta^\alpha \lambda^\alpha m_4}{\epsilon^\alpha m_5 m_3} + \frac{\lambda^\alpha \rho^\alpha}{m_5 m_3} \right) \times \left(\frac{\Lambda^\alpha(\phi^\alpha + \mu^\alpha + \gamma^\alpha \psi^\alpha)}{\mu^\alpha(\mu^\alpha + \phi^\alpha + \psi^\alpha)} \right) - 1 \right] \\
 & \quad \times \left[\beta_1^\alpha I(t) + \beta_2^\alpha D(t) + \lambda^\alpha P(t) \right] \\
 & = \left[\mathcal{R}_0 - 1 \right] \left[\beta_1^\alpha I(t) + \beta_2^\alpha D(t) + \lambda^\alpha P(t) \right].
 \end{aligned} \tag{11}$$

264

265 Therefore, $D_{t_0}^\alpha \mathcal{V}(t) < 0$ holds if $\mathcal{R}_0 < 1$. Furthermore if $\mathcal{R}_0 = 1$, $D_{t_0}^\alpha \mathcal{V}(t) = 0$ if and only
 266 if $S(t) = S^0, E(t) = E^0, I(t) = D(t) = P(t) = 0$. Thus, the largest compact invariant
 267 set in $U_1 = \{(S^0, E^0, 0, 0, 0) \in \Gamma : D_{t_0}^\alpha \mathcal{V}(t) = 0\}$ is a singleton set containing the disease-free
 268 equilibrium \mathcal{E}^0 . Therefore, by Theorem (3.3), we conclude that the disease-free equilibrium is
 269 globally asymptotically stable in Γ . \square

270 Next, we investigate the global stability of the endemic equilibrium point \mathcal{E}^* of model (10)
 271 when $\mathcal{R}_0 > 1$.

272 **Theorem 3.5.** For $\alpha \in (0, 1]$, whenever $\mathcal{R}_0 > 1$, then model (10) has a globally asymptotically
 273 stable endemic equilibrium point \mathcal{E}^* .

274 *Proof.* Let us consider the following appropriate Lyapunov function:

$$\begin{aligned}
 \mathcal{W}(t) & = \left\{ S(t) - S^* - S^* \ln \left(\frac{S(t)}{S^*} \right) \right\} + \left\{ E(t) - E^* - E^* \ln \left(\frac{E(t)}{E^*} \right) \right\} \\
 & \quad + \left\{ I(t) - I^* - I^* \ln \left(\frac{I(t)}{I^*} \right) \right\} + \frac{[\beta_2^\alpha D^* (\rho^\alpha I^* + \theta^\alpha D^*) + \lambda^\alpha P^* \theta^\alpha D^*] (S^* + \gamma^\alpha E^*)}{m_4 I^* [\rho^\alpha I^* + \theta^\alpha D^*]} \\
 & \quad \times \left\{ D(t) - D^* - D^* \ln \left(\frac{D(t)}{D^*} \right) \right\} + \frac{\lambda^\alpha P^* (S^* + \gamma^\alpha E^*)}{[\rho^\alpha I^* + \theta^\alpha D^*]} \\
 & \quad \times \left\{ P(t) - P^* - P^* \ln \left(\frac{P(t)}{P^*} \right) \right\}
 \end{aligned} \tag{12}$$

275

276

277 The time fractional order derivatives of $\mathcal{W}(t)$ are given by:

$$\begin{aligned}
 D_{t_0}^\alpha \mathcal{W}(t) &= \left(1 - \frac{S^*}{S(t)}\right) D_{t_0}^\alpha S(t) + \left(1 - \frac{E^*}{E(t)}\right) D_{t_0}^\alpha E(t) + \left(1 - \frac{I^*}{I(t)}\right) D_{t_0}^\alpha I(t) \\
 &\quad + \frac{[\beta_2^\alpha D^*(\rho^\alpha I^* + \theta^\alpha D^*) + \lambda^\alpha P^* \theta^\alpha D^*]}{m_4 I^* [\rho^\alpha I^* + \theta^\alpha D^*]} \times (S^* + \gamma^\alpha E^*) \left(1 - \frac{D^*}{D(t)}\right) D_{t_0}^\alpha D(t) \\
 &\quad + \frac{\lambda^\alpha P^* (S^* + \gamma^\alpha E^*)}{[\rho^\alpha I^* + \theta^\alpha D^*]} \left(1 - \frac{P^*}{P(t)}\right) D_{t_0}^\alpha P(t). \tag{13}
 \end{aligned}$$

279 Substituting the appropriate derivatives according to equations (10), we have:

$$\begin{aligned}
 D_{t_0}^\alpha \mathcal{W}(t) &= \left\{1 - \frac{S^*}{S(t)}\right\} \left\{ \psi^\alpha S(t) - \gamma^\alpha (\beta_1^\alpha I(t) + \beta_2^\alpha D(t) + \lambda^\alpha P) E(t) - (\phi^\alpha + \mu^\alpha) E(t) \right\} \\
 &\quad + \left\{1 - \frac{E^*}{E(t)}\right\} \left\{ \psi^\alpha S(t) - \phi^\alpha E(t) - \mu^\alpha E - \gamma^\alpha \beta_1^\alpha I(t) E(t) - \gamma^\alpha \beta_2^\alpha D_1(t) E(t) \right\} \\
 &\quad + \left\{1 - \frac{I^*}{I(t)}\right\} \left\{ [(\beta_1^\alpha I(t) + \beta_2^\alpha D(t) + \lambda^\alpha P(t)) S(t) + \gamma^\alpha (\beta_1^\alpha I(t) + \beta_2^\alpha D(t) \right. \\
 &\quad \left. + \lambda^\alpha P) E(t)] \right. \\
 &\quad \left. - (\mu^\alpha + \sigma^\alpha + \delta^\alpha) I(t) \right\} + \frac{[\beta_2^\alpha D^*(\rho^\alpha I^* + \theta^\alpha D^*) + \lambda^\alpha P^* \theta^\alpha D^*] (S^* + \gamma^\alpha E^*)}{m_4 I^* [\rho^\alpha I^* + \theta^\alpha D^*]} \\
 &\quad \times \left\{1 - \frac{D^*}{D(t)}\right\} \left\{ (\mu^\alpha + \delta^\alpha) I(t) - \epsilon^\alpha D(t) \right\} + \frac{\lambda^\alpha P^* (S^* + \gamma^\alpha E^*)}{[\rho^\alpha I^* + \theta^\alpha D^*]} \left\{1 - \frac{P^*}{P(t)}\right\} \\
 &\quad \times \left\{ \rho^\alpha I(t) + \theta^\alpha D(t) - (\tau^\alpha + \eta^\alpha) P(t) \right\}. \tag{14}
 \end{aligned}$$

282 At endemic equilibrium, we have:

$$\left\{ \begin{aligned}
 \Lambda^\alpha &= \beta_1^\alpha I^* S^* + \beta_2^\alpha D^* S^* + \lambda^\alpha P^* S^* + \mu^\alpha S^* + \psi^\alpha S^* - \phi^\alpha E^*, \\
 \psi^\alpha S^* &= \phi^\alpha E^* + \mu^\alpha E^* + \gamma^\alpha \beta_1^\alpha I^* E(t) + \gamma^\alpha \beta_2^\alpha D^* E^* + \gamma^\alpha \lambda^\alpha P^* E^*, \\
 (\mu^\alpha + \sigma^\alpha + \delta^\alpha) I^* &= \beta_1^\alpha I^* S^* + \beta_2^\alpha D^* S^* + \lambda^\alpha P^* S^* + \gamma^\alpha \beta_1^\alpha I^* E^* + \gamma^\alpha \beta_2^\alpha D^* E^* \\
 &\quad + \gamma^\alpha \lambda^\alpha P^* E^*, \\
 \epsilon^\alpha D^* &= (\mu^\alpha + \delta^\alpha) I^*, \\
 (\tau^\alpha + \eta^\alpha) P^* &= \rho^\alpha I^* + \theta^\alpha D^*.
 \end{aligned} \right. \tag{15}$$

284 Using the above constants at endemic equilibrium, we have:

$$\begin{aligned}
 D_{t_0}^\alpha \mathcal{W}(t) &= (\mu^\alpha + \beta_1^\alpha I^*) S^* \left\{ 2 - \frac{S(t)}{S^*} - \frac{S^*}{S(t)} \right\} + (\mu^\alpha + \gamma^\alpha \beta_1^\alpha I^*) E^* \left\{ 3 - \frac{S(t)}{S^*} \cdot \frac{E^*}{E(t)} \right. \\
 &\quad \left. - \frac{S^*}{S(t)} - \frac{E(t)}{E^*} \right\} + \phi^\alpha E^* \left\{ 2 - \frac{S(t)}{S^*} \cdot \frac{E^*}{E(t)} - \frac{S^*}{S(t)} \cdot \frac{E(t)}{E^*} \right\}
 \end{aligned}$$

$$\begin{aligned}
 & + \frac{\lambda^\alpha P^* S^* \rho^\alpha I^*}{(\rho^\alpha I^* + \theta^\alpha D^*)} \left\{ 3 - \frac{S^*}{S(t)} - \frac{I(t)}{I^*} \cdot \frac{P^*}{P(t)} - \frac{P(t)}{P^*} \cdot \frac{I^*}{I(t)} \cdot \frac{S(t)}{S^*} \right\} \\
 & + \frac{\gamma^\alpha \lambda^\alpha P^* E^* \rho^\alpha I^*}{(\rho^\alpha I^* + \theta^\alpha D^*)} \left\{ 4 - \frac{S^*}{S(t)} - \frac{I(t)}{I^*} \cdot \frac{P^*}{P(t)} - \frac{S(t)}{S^*} \cdot \frac{E^*}{E(t)} - \frac{P(t)}{P^*} \cdot \frac{I^*}{I(t)} \cdot \frac{E(t)}{E^*} \right\} \\
 & + \frac{\lambda^\alpha P^* S^* \theta^\alpha D^*}{(\rho^\alpha I^* + \theta^\alpha D^*)} \left\{ 4 - \frac{S^*}{S(t)} - \frac{I(t)}{I^*} \cdot \frac{D^*}{D(t)} - \frac{D(t)}{D^*} \cdot \frac{P^*}{P(t)} - \frac{P(t)}{P^*} \cdot \frac{I^*}{I(t)} \cdot \frac{S(t)}{S^*} \right\} \\
 & + \frac{\gamma^\alpha \lambda^\alpha P^* E^* \theta^\alpha D^*}{(\rho^\alpha I^* + \theta^\alpha D^*)} \left\{ 5 - \frac{S^*}{S(t)} - \frac{I(t)}{I^*} \cdot \frac{D^*}{D(t)} - \frac{D(t)}{D^*} \cdot \frac{P^*}{P(t)} - \frac{S(t)}{S^*} \cdot \frac{E^*}{E(t)} \right. \\
 & \left. - \frac{P(t)}{P^*} \cdot \frac{I^*}{I(t)} \cdot \frac{E(t)}{E^*} \right\} + \beta_2^\alpha S^* D^* \left\{ 3 - \frac{S^*}{S(t)} - \frac{I(t)}{I^*} \cdot \frac{D^*}{D(t)} - \frac{D(t)}{D^*} \cdot \frac{I^*}{I(t)} \cdot \frac{S(t)}{S^*} \right\} \\
 & + \gamma^\alpha \beta_2^\alpha E^* D^* \left\{ 4 - \frac{S^*}{S(t)} - \frac{S(t)}{S^*} \cdot \frac{E^*}{E(t)} - \frac{I(t)}{I^*} \cdot \frac{D^*}{D(t)} - \frac{D(t)}{D^*} \cdot \frac{I^*}{I(t)} \cdot \frac{E(t)}{E^*} \right\}. \quad (16)
 \end{aligned}$$

285

286 By the property that the arithmetic mean is greater than or equal to the geometric mean:

$$2 \leq \frac{S(t)}{S^*} + \frac{S^*}{S(t)}, \quad 2 \leq \frac{S(t)}{S^*} \cdot \frac{E^*}{E(t)} + \frac{S^*}{S(t)} \cdot \frac{E(t)}{E^*}, \quad 3 \leq \frac{S(t)}{S^*} \cdot \frac{E^*}{E(t)} + \frac{S^*}{S(t)} + \frac{E(t)}{E^*},$$

287

288

$$3 \leq \frac{S^*}{S(t)} + \frac{I(t)}{I^*} \cdot \frac{P^*}{P(t)} + \frac{P(t)}{P^*} \cdot \frac{I^*}{I(t)} \cdot \frac{S(t)}{S^*},$$

289

290

$$4 \leq \frac{S^*}{S(t)} + \frac{I(t)}{I^*} \cdot \frac{P^*}{P(t)} + \frac{S(t)}{S^*} \cdot \frac{E^*}{E(t)} + \frac{P(t)}{P^*} \cdot \frac{I^*}{I(t)} \cdot \frac{E(t)}{E^*},$$

291

292

$$4 \leq \frac{S^*}{S(t)} + \frac{I(t)}{I^*} \cdot \frac{D^*}{D(t)} + \frac{D(t)}{D^*} \cdot \frac{P^*}{P(t)} + \frac{P(t)}{P^*} \cdot \frac{I^*}{I(t)} \cdot \frac{S(t)}{S^*},$$

293

294

$$5 \leq \frac{S^*}{S(t)} + \frac{I(t)}{I^*} \cdot \frac{D^*}{D(t)} + \frac{D(t)}{D^*} \cdot \frac{P^*}{P(t)} + \frac{S(t)}{S^*} \cdot \frac{E^*}{E(t)} + \frac{P(t)}{P^*} \cdot \frac{I^*}{I(t)} \cdot \frac{E(t)}{E^*},$$

295

296

$$3 \leq \frac{S^*}{S(t)} + \frac{I(t)}{I^*} \cdot \frac{D^*}{D(t)} + \frac{D(t)}{D^*} \cdot \frac{I^*}{I(t)} \cdot \frac{S(t)}{S^*},$$

297

298

$$4 \leq \frac{S^*}{S(t)} + \frac{S(t)}{S^*} \cdot \frac{E^*}{E(t)} + \frac{I(t)}{I^*} \cdot \frac{D^*}{D(t)} + \frac{D(t)}{D^*} \cdot \frac{I^*}{I(t)} \cdot \frac{E(t)}{E^*},$$

299

300 for all $S(t) > 0$, $E(t) > 0$, $I(t) > 0$, $D(t) > 0$ and $P(t) > 0$, because the arithmetic mean is

301 greater than or equal to the geometric mean. Hence $\mathcal{W}(t) \leq 0$ and consequently, $D_{t_0}^\alpha \mathcal{W}(t) \leq 0$.

302 Moreover, the largest compact invariant set in $U_2 = \{(S^*, E^*, I^*, D^*, P^*) \in \Gamma : D_{t_0}^\alpha \mathcal{W}(t) = 0\}$

303 is a singleton set containing the endemic equilibrium \mathcal{E}^* , where $S(t) \equiv S^*$, $E(t) \equiv E^*$, $I(t) \equiv I^*$,

304 $D(t) \equiv D^*$, and $P(t) \equiv P^*$. Using Theorem (3.3), we conclude that the endemic equilibrium

305 point \mathcal{E}^* is globally asymptotically stable if $\mathcal{R}_0 > 1$. □

306 4 Numerical Simulations and Discussions

307 In this section, we performed the numerical simulations of the model (2) to justify the analytical
 308 results. Most of the parameter values which are not available in literature have been estimated
 309 within the reasonable realistic situation, the cumulative number of EVD monthly cases from
 310 March to August of the 2014 Ebola outbreak in Guinea was utilized (see [9]). We performed
 311 the numerical simulations using fractional Adam-Bashforth-Moulton scheme [43] as illustrated
 312 in equation (17):

313 For any differential equation:

$$314 \quad D_{t_0}^\alpha x(t) = g(t, x(t)), \quad 0 \leq t \leq T, \quad (17)$$

315 with the following initial conditions:

$$316 \quad x^i(0) = x_0^i, \quad i = 0, 1, 2, 3, \dots, [\alpha] - 1. \quad (18)$$

317 Operating by the fractional integral operator on equation (17) we obtain the solution $x(t)$ by
 318 solving equation (19):

$$319 \quad x(t) = \sum_{i=0}^{[\alpha]-1} \frac{x_0^i}{i!} t^i + \frac{1}{\Gamma(\alpha)} \int_0^t (t - \tau)^{\alpha-1} g(\tau, x(\tau)) d\tau. \quad (19)$$

320 Diethelm [54] used the predictor-corrector scheme based on the Adam-Bashforth-Moulton algo-
 321 rithm to numerically solve equation (19). Setting $h = \frac{T}{N}$, $t_n = nh$, and $n = 0, 1, 2, 3, \dots, N \in \mathbb{Z}^+$,
 322 we discretized equation (19) as a fractional variant of the one step Adam-Bashforth-Moulton
 323 scheme as shown in equation (20):

$$324 \quad x_h(t_{n+1}) = \sum_{i=0}^{|\alpha|-1} \frac{x_0^i}{i!} t_{n+1}^i + \frac{h^\alpha}{\Gamma(\alpha + 2)} \sum_{q=0}^n a_{q,n+1} g(t_q, x_q) \\ + \frac{h^\alpha}{\Gamma(\alpha + 2)} g(t_{n+1}, x_{n+1}^p), \quad (20)$$

$$\text{where: } a_{q,n+1} = \begin{cases} n^{\alpha+1} - (n - \alpha)(n + \alpha)^\alpha, & q = 0, \\ (n - q + 2)^{\alpha+1} + (n - q)^{\alpha+1} - 2(n - q + 1)^{\alpha+1}, & 1 \leq q \leq n, \\ 1, & q = n + 1, \end{cases}$$

325 and the predicted value $x_h^p(t_{n+1})$ is determined by:

$$326 \quad x_h(t_{n+1}) = \sum_{i=0}^{|\alpha|-1} \frac{x_0^i}{i!} t_{n+1}^i + \frac{1}{\Gamma(\alpha)} \sum_{q=0}^n b_{q,n+1} g(t_q, x_h(t_q)), \quad (21)$$

328 with:

$$329 \quad b_{q,n+1} = \frac{h^\alpha}{\alpha} ((n+1-q)^\alpha - (n-q)^\alpha). \quad (22)$$

330 The error estimate is:

$$331 \quad \max_{0 \leq q \leq k} |x(t_q) - x_h(t_q)| = O(h^p), \quad (23)$$

332 with $k \in \mathbb{N}$ and $p = \min(2, 1 + \alpha)$.

333 **4.1 Application of Adam-Bashforth-Moulton Scheme to the proposed mod-** 334 **el**

335 Most of the fractional order derivatives $\alpha \in (0, 1)$ that describe the real-world problems are
336 highly complicated and difficult to obtain its numerical approximations due to the existence of
337 their non-local in nature compared to the integer order derivatives. Adam-Bashforth-Moulton
338 scheme have been recognized as a powerful numerical scheme to solve nonlinear fractional order
339 problems due to its stability compared to other methods. Therefore, in this section we utilize
340 the Adam-Bashforth-Moulton scheme to numerically solve the nonlinear fractional model (2).
341 In the view to the generalized Adam-Bashforth-Moulton scheme, the proposed model (2) has
342 the following form:

343

$$\left. \begin{aligned}
 S(t_{n+1}) &= S_0 + \frac{h^\alpha}{\Gamma(\alpha + 2)} (\Lambda^\alpha - (\beta_1^\alpha I^p(t_{n+1}) + \beta_2^\alpha D^p(t_{n+1}) + \lambda^\alpha P^p(t_{n+1})) S^p(t_{n+1}) \\
 &\quad + \phi^\alpha E^p(t_{n+1}) - m_1 S^p(t_{n+1})) \\
 &\quad + \frac{h^\alpha}{\Gamma(\alpha + 2)} \sum_{q=0}^n a_{q,n+1} (\Lambda^\alpha - (\beta_1^\alpha I(t_q) + \beta_2^\alpha D(t_q) + \lambda^\alpha P(t_q)) S(t_q) \\
 &\quad + \phi^\alpha E(t_q) - m_1 S(t_q)), \\
 E(t_{n+1}) &= E_0 + \frac{h^\alpha}{\Gamma(\alpha + 2)} (\psi^\alpha S^p(t_{n+1}) - \gamma^\alpha (\beta_1^\alpha I^p(t_{n+1}) + \beta_2^\alpha D^p(t_{n+1})) \\
 &\quad + \lambda^\alpha P^p(t_{n+1})) E^p(t_{n+1}) - m_2 E^p(t_{n+1})) \\
 &\quad + \frac{h^\alpha}{\Gamma(\alpha + 2)} \sum_{q=0}^n a_{q,n+1} (\psi^\alpha S(t_q) - \gamma^\alpha (\beta_1^\alpha I(t_q) + \beta_2^\alpha D(t_q)) \\
 &\quad + \lambda^\alpha P(t_q)) E(t_q) - m_2 E(t_q)), \\
 I(t_{n+1}) &= I_0 + \frac{h^\alpha}{\Gamma(\alpha + 2)} ([(\beta_1^\alpha I^p(t_{n+1}) + \beta_2^\alpha D^p(t_{n+1}) + \lambda^\alpha P^p(t_{n+1})) S^p(t_{n+1}) \\
 &\quad + \gamma^\alpha (\beta_1^\alpha I^p(t_{n+1}) + \beta_2^\alpha D^p(t_{n+1}) + \lambda^\alpha P^p(t_{n+1})) E^p(t_{n+1})] - m_3 I^p(t_{n+1})) \\
 &\quad + \frac{h^\alpha}{\Gamma(\alpha + 2)} \sum_{q=0}^n a_{q,n+1} ([(\beta_1^\alpha I(t_q) + \beta_2^\alpha D(t_q) + \lambda^\alpha P(t_q)) S(t_q) \\
 &\quad + \gamma^\alpha (\beta_1^\alpha I(t_q) + \beta_2^\alpha D(t_q) + \lambda^\alpha P(t_q)) E(t_q)] - m_3 I(t_q)) \\
 R(t_{n+1}) &= R_0 + \frac{h^\alpha}{\Gamma(\alpha + 2)} (\sigma^\alpha I^p(t_{n+1}) - \mu^\alpha R^p(t_{n+1})) \\
 &\quad + \frac{h^\alpha}{\Gamma(\alpha + 2)} \sum_{q=0}^n a_{q,n+1} (\sigma^\alpha I(t_q) - \mu^\alpha R(t_q)) \\
 D(t_{n+1}) &= D_0 + \frac{h^\alpha}{\Gamma(\alpha + 2)} (m_4 I^p(t_{n+1}) - \epsilon^\alpha D^p(t_{n+1})) \\
 &\quad + \frac{h^\alpha}{\Gamma(\alpha + 2)} \sum_{q=0}^n a_{q,n+1} (m_4 I(t_q) - \epsilon^\alpha D(t_q)) \\
 P(t_{n+1}) &= P_0 + \frac{h^\alpha}{\Gamma(\alpha + 2)} (\rho^\alpha I^p(t_{n+1}) + \theta^\alpha D^p(t_{n+1}) - m_5 P^p(t_{n+1})) \\
 &\quad + \frac{h^\alpha}{\Gamma(\alpha + 2)} \sum_{q=0}^n a_{q,n+1} (\rho^\alpha I(t_q) + \theta^\alpha D(t_q) - m_5 P(t_q)),
 \end{aligned} \right\} (24)$$

344

345 where:

$$\left. \begin{aligned}
 S^p(t_{n+1}) &= S_0 + \frac{h^\alpha}{\Gamma(\alpha)} \sum_{q=0}^n b_{q,n+1} (\Lambda^\alpha - (\beta_1^\alpha I(t_q) + \beta_2^\alpha D(t_q) + \lambda^\alpha P(t_q)) S(t_q) \\
 &\quad + \phi^\alpha E(t_q) - m_1 S(t_q)), \\
 E^p(t_{n+1}) &= E_0 + \frac{h^\alpha}{\Gamma(\alpha)} \sum_{q=0}^n b_{q,n+1} (\psi^\alpha S(t_q) - \gamma^\alpha (\beta_1^\alpha I(t_q) + \beta_2^\alpha D(t_q) \\
 &\quad + \lambda^\alpha P(t_q)) E(t_q) - m_2 E(t_q)), \\
 I^p(t_{n+1}) &= I_0 + \frac{h^\alpha}{\Gamma(\alpha)} \sum_{q=0}^n b_{q,n+1} ((\beta_1^\alpha I(t_q) + \beta_2^\alpha D(t_q) + \lambda^\alpha P(t_q)) S(t_q) \\
 &\quad + \gamma^\alpha (\beta_1^\alpha I(t_q) + \beta_2^\alpha D(t_q) + \lambda^\alpha P(t_q)) E(t_q)) - m_3 I(t_q)), \\
 R^p(t_{n+1}) &= R_0 + \frac{h^\alpha}{\Gamma(\alpha)} \sum_{q=0}^n b_{q,n+1} (\sigma^\alpha I(t_q) - \mu^\alpha R(t_q)) \\
 D^p(t_{n+1}) &= D_0 + \frac{h^\alpha}{\Gamma(\alpha)} \sum_{q=0}^n b_{q,n+1} (m_4 I(t_q) - \epsilon^\alpha D(t_q)) \\
 P^p(t_{n+1}) &= P_0 + \frac{h^\alpha}{\Gamma(\alpha)} \sum_{q=0}^n b_{q,n+1} (\rho^\alpha I(t_q) + \theta^\alpha D(t_q) - m_5 P(t_q)).
 \end{aligned} \right\} \quad (25)$$

346

347 In simulating the model (2) we assume the initial condition that $S(0) = 10000$, $E(0) =$
 348 290 , $I(0) = 10$, $R(0) = 50$, $D(0) = 0$ and $P(0) = 0$.

Table 2: Parameters and values

Symbol	Definition	Range/ Value	Units	Source
δ	Disease death rate	0.4-0.9	day^{-1}	[46, 55, 56]
η	Environmental decontamination rate	0.06	day^{-1}	fitted
β_1	Transmission rate of infectious humans	variable	day^{-1}	[55, 57, 58]
β_2	Transmission rate of deceased humans	variable	day^{-1}	[56, 58]
λ	Transmission rate of Ebola virus	variable	day^{-1}	fitted
τ	Pathogen decay rate	$(0, \infty)$	day^{-1}	[59, 60]
ρ	Shading rate of infectious humans	0.0004	day^{-1}	fitted
θ	Shading rate of deceased humans	0.004	day^{-1}	fitted
ϵ	Burial rate of deceased humans	$(0, 1)$	day^{-1}	[58, 61]
μ	Natural death rate	$(0, 1)$	day^{-1}	[62]
ϕ	Lost of education rate	0.025	day^{-1}	fitted
γ	Modification factor	0.7	-	fitted
Λ	Recruitment rate	variable	day^{-1}	fitted
ψ	Education rate	0.31	day^{-1}	fitted
σ	Recovery rate of humans	$(0, 1)$	day^{-1}	[55, 57, 58]

349 4.2 Sensitivity Analysis

350 In this section, we perform the sensitivity analysis of the model (2). The threshold quantity \mathcal{R}_0
351 known as basic reproduction number is an important parameter to determine the persistence
352 and extinction of EVD in the population. Parameter values of the Ebola model in Equation
353 (2) taken from literature as presented in Table 2 and while some are estimated, therefore,
354 sensitivity analysis will be useful on identifying parameters with greatest influence to change
355 the magnitude of threshold quantity \mathcal{R}_0 .

356 **Definition 2.** (See, [63]) *The normalized sensitivity index of \mathcal{R}_0 which depends on differen-*
357 *tiability of parameter ω is defined as equation (26):*

358

$$\Psi_{\omega}^{\mathcal{R}_0} = \frac{\partial \mathcal{R}_0}{\partial \omega} \times \frac{\omega}{\mathcal{R}_0}, \quad (26)$$

359

360 where ω is the generic parameter of system (2).

Table 3: Sensitivity index of the model (2)

Parameter	β_1	β_2	λ	ϕ
Index	+0.4154	+0.371	+0.2125	+0.0106
Parameter	σ	δ	ρ	θ
Index	-0.0107	-0.2939	+0.0023	+0.2102
Parameter	ψ	μ	γ	
Index	-0.0154	-0.1054	-0.1579	
Parameter	τ	η	ϵ	
Index	-0.008	0	-0.5823	

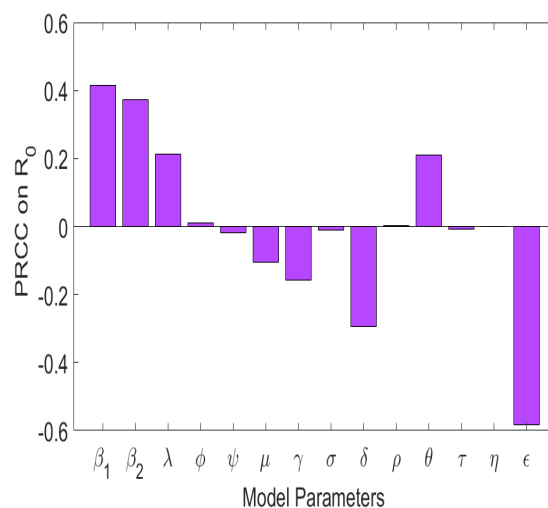


Figure 2: Sensitivity index of the model (2)

361 We observed that model parameters such as β_1 , β_2 , λ , ϕ , ρ , and θ , have a positive influence
 362 on the magnitude of \mathcal{R}_0 , that is, whenever they are increased, the magnitude of \mathcal{R}_0 increases.
 363 In Figure 2 it can be observed that an increase in the values of β_1 , β_2 , λ , ϕ , ρ , and θ by
 364 10% increases the magnitude of \mathcal{R}_0 by 4.154%, 3.721%, 2.125%, 0.106%, 0.023%, and 2.102%,
 365 respectively. While model parameters with negative index values have a negative influence on
 366 the magnitude of \mathcal{R}_0 an increase in the values of ψ , μ , γ , σ , δ , τ and ϵ by 10% decreases the
 367 magnitude of \mathcal{R}_0 by 0.154%, 1.054%, 1.579%, 0.107%, 2.939%, 0.08%, and 5.823%, respectively.
 368 These results suggest that the burial rate of deceased humans ϵ , has the highest negative
 369 influence on the magnitude of \mathcal{R}_0 . In addition, an increase in the indirect transmission rate of

370 Ebola virus λ , increases the magnitude of \mathcal{R}_0 .

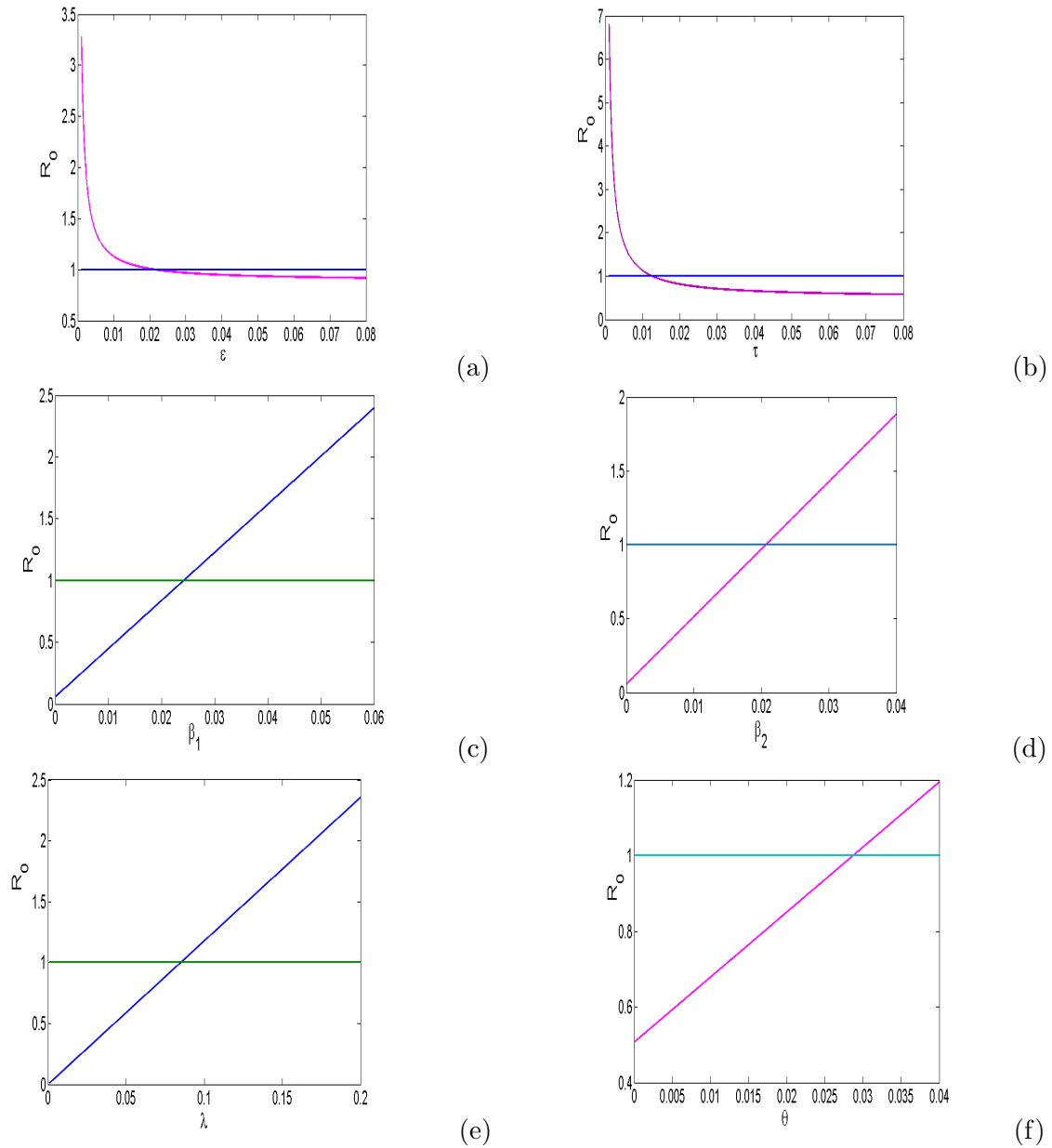


Figure 3: Numerical results of model (2) showing effects of varying (a) burial rate of deceased humans ϵ , on \mathcal{R}_0 (b) pathogen decay rate of Ebola virus τ , on \mathcal{R}_0 (c) transmission rate from infectious human β_1 , on \mathcal{R}_0 (d) transmission rate of deceased humans β_2 , on \mathcal{R}_0 (e) transmission rate of Ebola virus λ , on \mathcal{R}_0 (f) shading rate of deceased humans θ , on \mathcal{R}_0 .

371 We simulated model (2) to evaluate the effects of (a) burial rate of deceased humans ϵ , on
 372 \mathcal{R}_0 , at different values of ϵ , (b) pathogen decay rate of Ebola virus τ , on \mathcal{R}_0 , at different
 373 values of τ , (c) transmission rate from infectious human β_1 , on \mathcal{R}_0 , at different values of β_1

374 (d) transmission rate of deceased humans β_2 , on \mathcal{R}_0 , at different values of β_2 , (e) transmission
 375 rate of Ebola virus λ , on \mathcal{R}_0 , at different values of λ (f) shading rate of deceased humans θ ,
 376 on \mathcal{R}_0 , at different values of θ . The other parameters are fixed in all cases as in Table 3.
 377 The numerical results in Figure 3 (a) show burial rate of deceased humans ϵ , on \mathcal{R}_0 . We noted
 378 that increasing the burial rate on the deceased humans reduces the size of \mathcal{R}_0 . Additionally,
 379 whenever ϵ is greater than 0.02, the EVD dies in the community. In Figure 3 (b), we assess
 380 the effect of pathogen decay rate of Ebola virus τ , on \mathcal{R}_0 . We noted that whenever $\tau > 0.01$,
 381 the disease dies in the population. The numerical results in Figure 3 (c) show transmission
 382 rate from infectious β_1 , on \mathcal{R}_0 . We noted that increasing the transmission rate from infectious
 383 human increases the magnitude of \mathcal{R}_0 . In particular, whenever β_1 is greater than 0.025, the
 384 disease persists in the community. In Figure 3 (d), we investigated the influence of transmission
 385 rate of deceased humans β_2 , on \mathcal{R}_0 . We observed that whenever $\beta_2 > 0.02$, the disease persists
 386 in the population. The numerical results in Figure 3 (e) show transmission rate of Ebola virus
 387 λ , on \mathcal{R}_0 . We observed that increasing the transmission rate of Ebola virus increases the size
 388 of \mathcal{R}_0 . In particular, whenever λ is greater than 0.1, the disease persists in the community. In
 389 Figure 3 (f), we investigated the influence of shading rate of deceased humans θ , on \mathcal{R}_0 . We
 390 noted that whenever $\theta > 0.03$, the disease persists in the community.

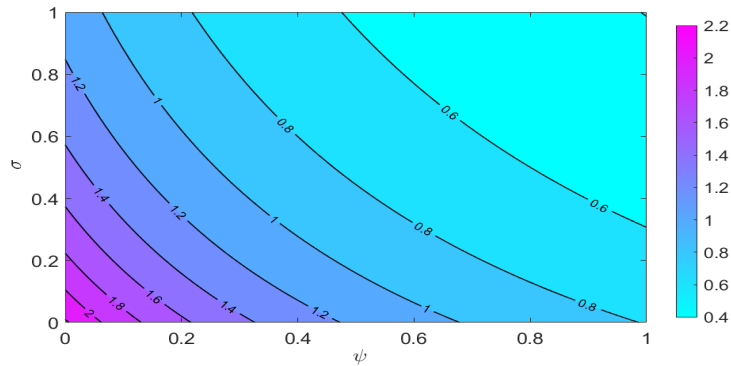


Figure 4: Numerical results of model (2) showing contour graph of \mathcal{R}_0 as the function of prevention measures and educational campaigns. We simulated the model (2) at $\epsilon = 0.074$, $\phi = 0.0004$, $\beta_1 = 1 \times 10^{-8}$, and $\beta_2 = 9.7 \times 10^{-6}$.

391 Figure 4 shows the contour graph of \mathcal{R}_0 as the function of educational campaigns and prevention
 392 measures. We simulated the model (2) at $\epsilon = 0.074$, $\phi = 0.0004$, $\beta_1 = 1 \times 10^{-8}$, and
 393 $\beta_2 = 9.7 \times 10^{-6}$. The results showed that as the rate of prevention measures and educational
 394 campaigns increases, the value of \mathcal{R}_0 decreases. This shows that both prevention measures

395 and educational campaigns have the potential to reduce the spread of EVD in the community.

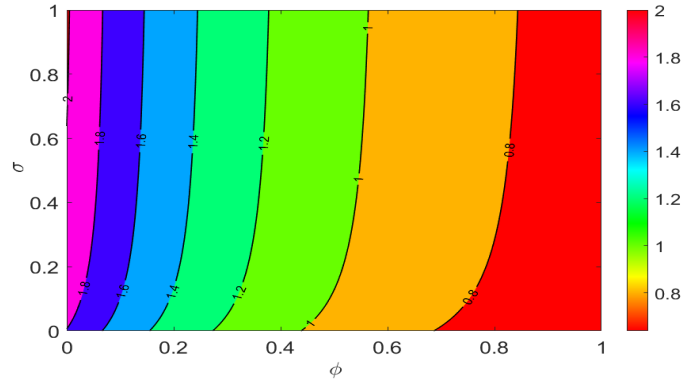


Figure 5: Numerical results of model (2) showing contour graph of \mathcal{R}_0 as the function of prevention measures and treatment of infected individuals. We simulated the model (2) at $\epsilon = 0.08$, $\psi = 0.025$, $\beta_1 = 1 \times 10^{-8}$, and $\beta_2 = 9.7 \times 10^{-6}$.

396 Figure 5 shows the contour graph of \mathcal{R}_0 as the function of prevention measures and recovery rate
 397 due to the treatment of infected individuals . We simulated the model (2) at $\epsilon = 0.08$, $\psi =$
 398 0.025 , $\beta_1 = 1 \times 10^{-8}$, and $\beta_2 = 9.7 \times 10^{-6}$. We observe that increasing the rate of prevention
 399 measures and recovery rate due to the treatment of infected individuals lead to decreased
 400 magnitude of \mathcal{R}_0 . This demonstrates the effect of prevention measures and treatment of
 401 infected individuals in reducing the transmission of Ebola in the population.

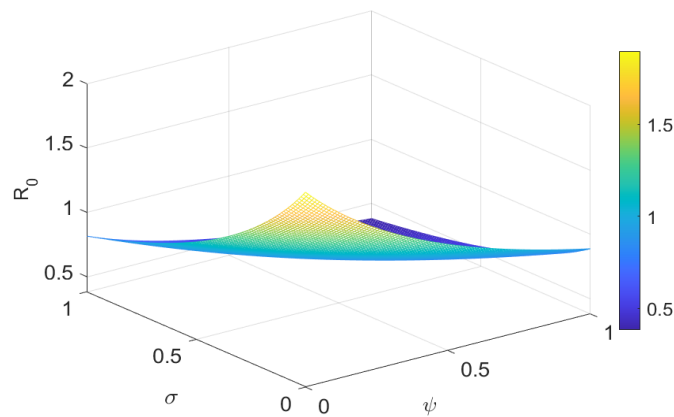


Figure 6: Mesh plot of \mathcal{R}_0 as the function of educational campaigns and recovery rate due to the treatment of infected individuals. We simulated the model (2) at $\epsilon = 0.094$, $\phi = 0.071$, $\beta_1 = 1 \times 10^{-8}$, and $\beta_2 = 9.7 \times 10^{-6}$.

402 Figure 6 shows the mesh plot of \mathcal{R}_0 as the function of educational campaigns and recovery rate
 403 due to the treatment of infected individuals . We simulated the model (2) at $\epsilon = 0.094$, $\phi =$
 404 0.071 , $\beta_1 = 1 \times 10^{-8}$, and $\beta_2 = 9.7 \times 10^{-6}$. It was noted that increasing the rate of educational
 405 campaigns and recovery rate due to the treatment of infected individuals lead to decreased
 406 magnitude of \mathcal{R}_0 . This demonstrates the effect of educational campaigns and treatment of
 407 infected individuals reduce the transmission of Ebola in the population.

408 4.3 Parameter Estimation

409 In this section, we numerically solve the proposed model (2) and estimate the parameters η ,
 410 $\lambda, \rho, \theta, \phi, \gamma, \Lambda, \psi$ that minimize the deviation of real data from the prediction model (2) using
 411 the least squares (RMSE) and Nelder mead algorithm techniques, and while the rest are fitted.
 412 The real data of Ebola cases used are reported in [9]. Despite the challenges in model fitting
 413 and parameter estimations, model fitting and parameter estimation in fractional order models
 414 is an integral part in the disease modeling. The present data were reported in Guinea from
 415 22 March to 16 August 2014, and the cumulative new infections predicted by the model (2) is
 416 obtained using the equation (27):

$$417 \quad D_{t_0}^\alpha C(t) = (\beta_1^\alpha I(t) + \beta_2^\alpha D(t) + \lambda^\alpha P(t))(S(t) + \gamma^\alpha E(t)) \quad (27)$$

418 Further, we use the following function to compute the best fitting:

$$419 \quad \mathbb{F} : \mathbb{R}_{(\eta, \lambda, \rho, \theta, \phi, \gamma, \Lambda, \psi)}^8 \rightarrow \mathbb{R}_{(\eta, \lambda, \rho, \theta, \phi, \gamma, \Lambda, \psi)} \quad (28)$$

420 where $\eta, \lambda, \rho, \theta, \phi, \gamma, \Lambda, \psi$ are variables such that:

421 (1) For a given $(\eta, \lambda, \rho, \theta, \phi, \gamma, \Lambda, \psi)$, solve numerically the model differential equations (2) to
 422 obtain a solution $\hat{Y}_i(t) = (\hat{S}, \hat{E}, \hat{I}, \hat{R}, \hat{P}, \hat{D})$ which is an approximation of the reported
 423 Ebola cases $Y(t)$.

424 (2) Set $t_0 = 1$ (the model fitting starts in March 22) and for $t = 2, 3, \dots, 53$, corresponding to
 425 the number of weeks where data are available, obtain the computed numerical solution
 426 for $i_h(t)$; that is., $\hat{I}(1), \hat{I}(2), \hat{I}(3), \dots, \hat{I}(53)$.

427 (3) Compute the (RMSE) of the difference between $\hat{I}(1), \hat{I}_h(2), \dots, \hat{I}_h(53)$ and observed cases.

428 This function \mathbb{F} yields the RMSE where

$$429 \quad \text{RMSE} = \sqrt{\frac{1}{n} \sum_{k=1}^{53} (I(k) - \hat{I}(k))^2}, \quad (29)$$

430 (4) By using Nelder-Mead algorithm determine a global minimum for the RMSE .

431 The function \mathbb{F} takes values in \mathbb{R}^8 and yields a positive real number, the RMSE that measures
 432 the closeness of the model predictions to the observed data. Using the formula in equation (29),
 433 the *RMSE* was found to be 0.1353. This shows that the proposed model had 13.53% deviations
 434 from observed values. It concluded that the model was approximately 86.47% efficient. On
 435 performing the fitting process, we assume the following initial conditions $S(0) = 1000$, $E(0) =$
 436 290 , $I(0) = 10$, $R(0) = 50$, $D(0) = 0$, and $P(0) = 0$ and the model parameters in Table (2).

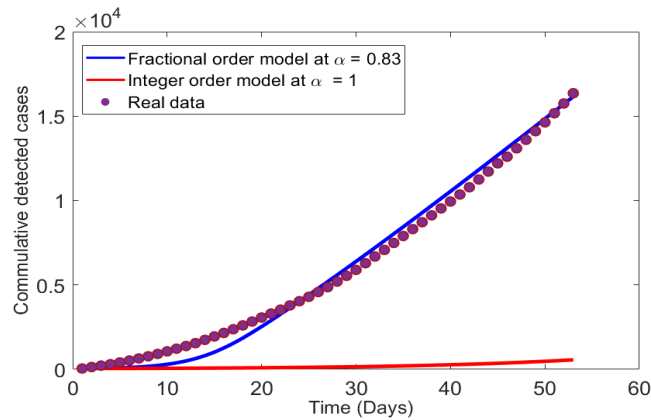


Figure 7: The model (2) fitted to Ebola cases reported in Guinea from 22 March to 16 August 2014 at $\alpha = 0.83$.

437 Figure 7 shows the cumulative detected cases of Ebola in Guinea. We used the monthly report
 438 of Ebola cases reported in [9] to fit the model (2) at $\alpha = 0.83$. The results demonstrated
 439 that the model (2) fits well the monthly Ebola cases reported in Guinea from 22 March to 16
 440 August 2014 .

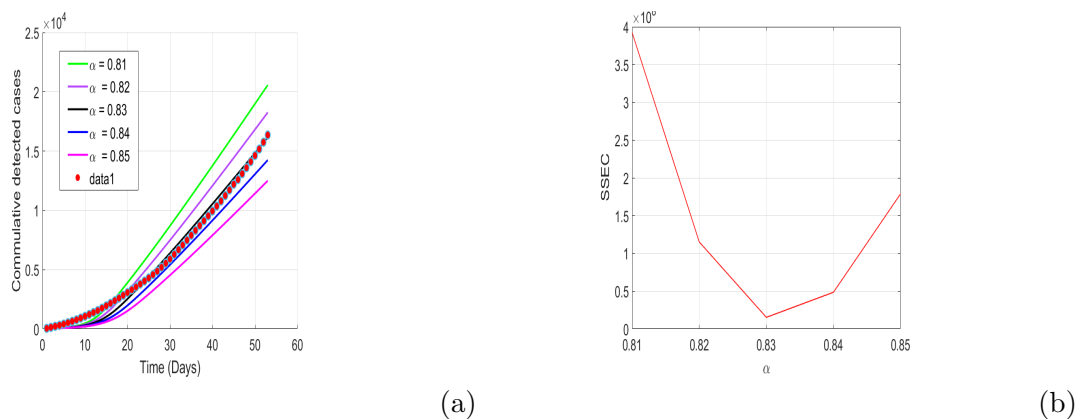


Figure 8: Numerical results of model 2 (a) shows the real data fitted at different order of derivatives (b) plots of order derivatives against the sum of square error cumulative (SSEC)

441 The numerical results in Figure 8 (a) shows the real data fitted with the fractional model at the
 442 order of derivatives $\alpha = 0.81, 0.82, 0.83, 0.84, 0.85$. We noted that the model had better fit at
 443 $\alpha = 0.83$. Figure (b), we plotted the variation of order of derivative against the sum of square
 444 error cumulative (SSEC). Overall, the model had minimum sum of square error cumulative at
 445 $\alpha = 0.83$ which agree with results in Figure (b). Thus, the model had better fits at $\alpha = 0.83$.

446 4.4 Numerical Results

447 Next, we simulate the model (2), we varied different model parameters and the order α of the
 448 caputo operator in order to explain the role of various parameters and memory index on the
 449 disease transmission patterns and control to support the analytical results. We first simulate
 450 the model at $\mathcal{R}_0 > 1$, followed by simulation at $\mathcal{R}_0 < 1$ to show the dynamics of the disease in
 451 the population.

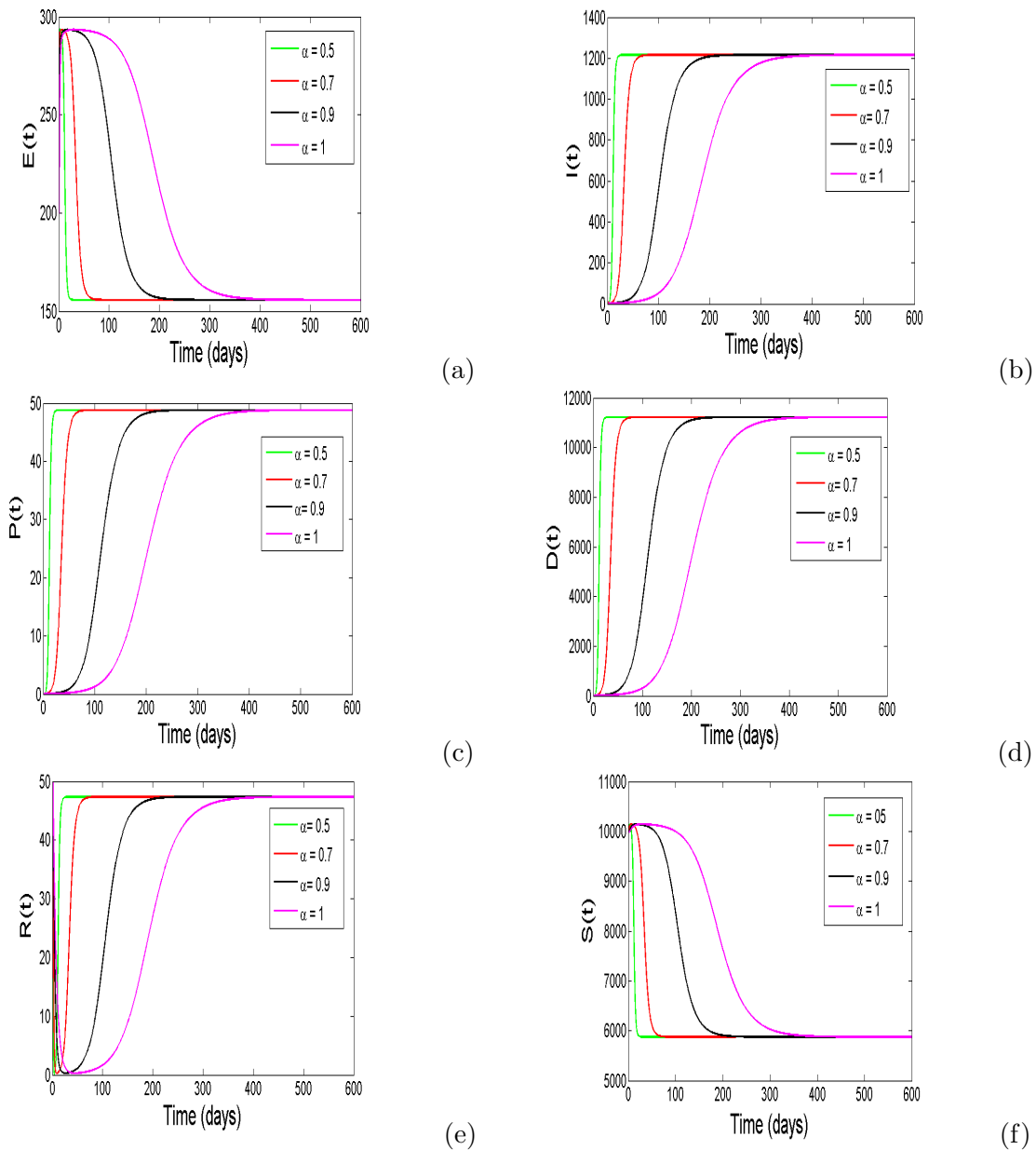


Figure 9: Simulation of the model (2) showing the convergence of infected individuals at the endemic equilibria point.

452 Figure 9 is a simulation of the model (2) to demonstrate the solution profile of individuals at
 453 the endemic equilibrium point. To explore the effects of different derivative orders, α , on the
 454 dynamics of the disease, we simulated the model at $\mathcal{R}_0 = 1.7520$, with the parameter values
 455 in Table 2 for $\alpha = 0.5$, $\alpha = 0.7$, $\alpha = 0.9$, and $\alpha = 1$. As we can note, with baseline
 456 values in Table 2, the disease will persist. Firstly, the results show that the variables for
 457 infected epidemiological compartments $I(t)$, $D(t)$, and $P(t)$ in Figure 9 (b), 9 (c), and 9 (d)

458 respectively, will increase the infection gradually and after about 300 days, the infection settle
 459 and attain stability at the endemic equilibrium at $I(t) \approx 1200$, $D(t) \approx 1050$, and $P(t) \approx 49$.
 460 A Similar pattern are observed for the compartment $R(t)$ in Figure (9)(e). In addition, the
 461 variables for susceptible epidemiological compartments $S(t)$, and $E(t)$ in Figure (9)(a), and
 462 (9)(f) respectively, show that susceptibility will decrease gradually and after about 300 days,
 463 the susceptibility settle and attain stability at the endemic equilibrium at $S(t) \approx 600$, and
 464 $E(t) \approx 290$. One can observe that as the value of the fractional-order α approaches unity,
 465 the time taken by model variables to converge to their respective unique endemic equilibrium
 466 point increases. These results agree with the analytical analysis of global stability for endemic
 467 equilibrium point in Theorem 3.4. It was further noted that at the fractional-order derivatives
 468 α , the human population attain its stability faster than at the classical integer.

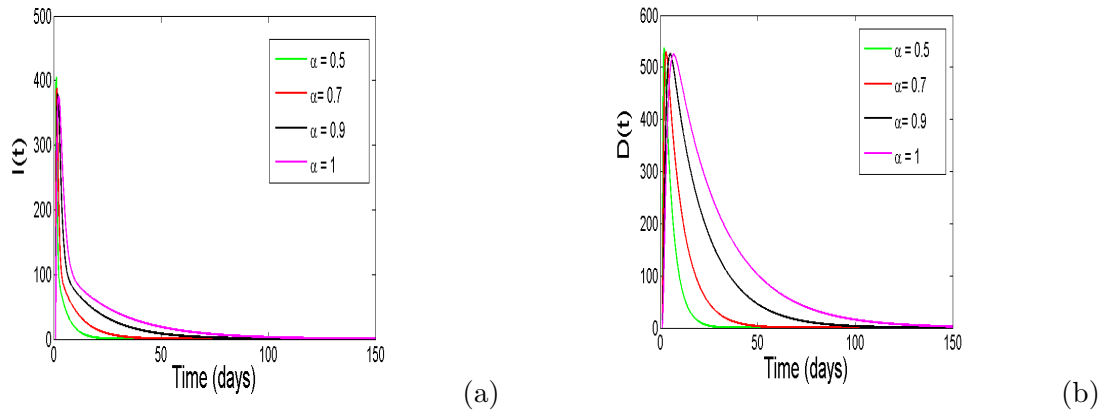


Figure 10: Simulation of the model (2) to show the convergence of infected humans and dead bodies at the disease free equilibrium point. We simulate the model (2) at $\mathcal{R}_0 = 0.6916$ with $\beta_1 = 1 \times 10^{-8}$, $\beta_2 = 9.7 \times 10^{-6}$, $\phi = 0.85$, $\psi = 0.71$. At different values of fractional-order derivatives, the number of infected individuals generated over the period of 150 days converge to the disease free equilibrium point.

469 Figure (10) shows the simulation of the model (2) to demonstrate the convergence of infected
 470 human population to the disease-free equilibrium point. To examine the effects of different
 471 derivative orders, α , on the dynamics of the disease, we simulated the model at $\mathcal{R}_0 = 0.6916$,
 472 with $\beta_1 = 1 \times 10^{-8}$, $\beta_2 = 9.7 \times 10^{-6}$, $\phi = 0.85$, $\psi = 0.71$ and the remainder retained the
 473 baseline values in Table 2 for $\alpha = 0.5$, $\alpha = 0.7$, $\alpha = 0.9$, and $\alpha = 1$. As we can note, with
 474 baseline values in Table 2, the disease will die. We can note that, the variables for infected epi-
 475 demiological compartments $I(t)$, and $D(t)$ in Figure 10 (a), and 10 (b), respectively, show that
 476 the infection will decrease gradually and after about 100 days, the infection settle and attain

477 stability at the disease-free equilibrium at $I(t) = 0$, and $D(t) = 0$. Furthermore, as the value of
 478 the fractional-order α approaches unity, the time taken by the model variables to converge to
 479 their respective unique disease-free equilibrium point increases. The results demonstrate that
 480 in a long-range interaction of people in the population, all infected individuals converge to one
 481 point which is the disease-free equilibrium point. This agrees with the analytical results on
 482 the existence of global stability for disease-free equilibrium point for the model (2) in Theorem
 483 3.5. Also we have noted that as the fractional-order derivatives α decrease from integer and
 484 infected humans attain stability much faster than at $\alpha = 1$. This shows the importance of
 485 using fractional-order derivatives in modeling biological systems.

486 5 Concluding Remarks

487 In this article, a Caputo derivative model for EVD with intervention strategies is proposed
 488 and analyzed. A Majority of mathematical models for EVD in literature are based on integer-
 489 ordinary differential equations, and much has not been done to investigate the role of memory
 490 effects on EVD dynamics. Thus, the main aim of this study was to develop a more realistic
 491 EVD model that incorporate memory effects. The formulated model subdivides the total
 492 human population based on epidemiological status as susceptible population unaware of the
 493 disease fighting, susceptible population aware of disease fighting; infected individuals who are
 494 clinically displaying signs of the disease and are infectious, individuals who have recovered
 495 from infection, and deceased population. The studied model has an additional compartment
 496 that captures the concentration of pathogens in the environment. We perform the sensitivity
 497 analysis to demonstrate the influence of each parameter on the magnitude of threshold quantity
 498 \mathcal{R}_0 . The results show that that model parameters such as β_1 , β_2 , λ , ϕ , ρ , and θ , have a positive
 499 correlation with the magnitude of \mathcal{R}_0 , that is, whenever they are increased, the magnitude
 500 of \mathcal{R}_0 increases. Furthermore, an increase in the values of β_1 , β_2 , λ , ϕ , ρ , and θ by 10%
 501 will increase the magnitude of \mathcal{R}_0 by 4.154%, 3.721%, 2.125%, 0.106%, 0.023%, and 2.102%,
 502 respectively. While model parameters with negative index values have a negative correlation
 503 with the magnitude of \mathcal{R}_0 , we observed that an increase in the values of ψ , μ , γ , σ , δ , τ and
 504 ϵ by 10% decreases the magnitude of \mathcal{R}_0 by 0.154%, 1.054%, 1.579%, 0.107%, 2.939%, 0.08%,
 505 and 5.823%, respectively. These results suggest that the burial rate of deceased humans ϵ , has
 506 the highest negative influence on the magnitude of \mathcal{R}_0 . In addition, an increase in the indirect
 507 transmission rate of Ebola virus λ , will increase the magnitude of \mathcal{R}_0 .

508 The analytical results obtained in this study demonstrate that the fractional-order model
509 has a globally asymptotically stable disease-free equilibrium whenever $\mathcal{R}_0 < 1$. However, if
510 $\mathcal{R}_0 > 1$, the fractional-order model has an endemic equilibrium which is globally asymptotically
511 stable.

512 Subsequently, we fitted the model parameters with the Ebola cases reported in Guinea from
513 22 March to 16 August 2014 at $\alpha = 0.82, 0.83, 0.84$ and 0.85 . From our numerical results,
514 the model fits well with cases reported and health education campaigns, prevention measures
515 and treatments have the potential to minimize the spread of Ebola in the population. As the
516 memory effect α decreases from unity, the solution profiles of the model (2) attain stability
517 much faster than at $\alpha = 1$. In addition, the different values of the fractional-order have no effect
518 on the stability of the model (2) but influence the time taken for stability to be attained. These
519 results demonstrate the importance of fractional-order over the classical integer in modeling
520 biological systems.

521 As the modelling of EVD is not sufficiently developed, this work offers many opportunities
522 in improvements for future research where the model can be extended to incorporate a patch
523 structure to account for the circulation of the disease in many countries as it is the case in
524 Western Africa. In addition we expect to improve this study in the future by developing EVD
525 model(s) with a time delay that will enable the comparison of the Caputo derivative and time
526 delay approach

527

536 **References**

- 537 [1] P. Rouguet, J.-M. Bermejo, A. Kilbourne, W. Karesh, P. Reed, B. Kumulunui, P. Yaba,
538 A. Delicat, P.E. Rollin, E.M. "Leroy, Wild animal mortality monitoring and human Ebola
539 outbreak, Gabon and republic of Congo, 2001-2003", *Emerg, infect. Dis*, 11,283-290,
540 2005.
- 541 [2] T. Smith, "Ebola and Marbug Virus (Deadly Disease and epidemics), second ed.",
542 *Chelsea House Pub*, 2010.
- 543 [3] WHO, "Ebola data and statistics," [http://apps.who.int/gho/data/view.ebola-sitrep.ebola-](http://apps.who.int/gho/data/view.ebola-sitrep.ebola-summary-20160511?lang=en.)
544 [summary-20160511?lang=en.](http://apps.who.int/gho/data/view.ebola-sitrep.ebola-summary-20160511?lang=en.), 2016.
- 545 [4] M.F. Jalloh, W. Li, R.F. Bunnell, et al, "Impact of Ebola experiences and risk perceptions
546 on mental health in Sierra Leone, July 2015", *BMJ Global Health*, 3:e000471, 2018.
- 547 [5] P. Richards, J. Amara, M.C. Ferme, P. Kamar, E. Mokuwa, A.I. Sheriff, R. Suluku , M.
548 Voors Marten, "Social pathways for Ebola virus disease in rural Sierra Leone and some
549 implications for containment", *PLOS Negl Trop Dis.*, 8(7):e3056, 2014.
- 550 [6] A. Manguvo, and B. Mafuvadze, "The impact of traditional and religious practices on
551 the spread of Ebola in West Africa: time for a strategic shift", *The Pan African medical*
552 *journal*, 22 Suppl 1(Suppl 1), 9. doi:10.11694/pamj.suppl.2015.22.1.6190, 2015.
- 553 [7] S. Hewlett Barry, P. Amola Richard, "Cultural contexts of Ebola in northern Uganda",
554 *Emerg Infect Dis.*; 9(10):1242, 2003.
- 555 [8] World Health Organization, "Global alert and response", 2014.
- 556 [9] C.L. Althaus, "Estimating the reproduction number of Ebola virus (EBOV) during the
557 2014 outbreak in West Africa", *PLoS Currents Outbreaks*, 6 (2014), 2014.
- 558 [10] M.V. Barbarossa, A. Denes, G. Kiss, Y. Nakata, G. Rost, & Z. Vizi, "Transmission
559 dynamics and final epidemic size of Ebola Virus Disease outbreaks with varying inter-
560 ventions", *PLoS One* ,10(7), e0131398, 2015.
- 561 [11] T. Berge, J.M.-S. Lubuma, G. M. Moremedi, N. Morris and R. Kondera-Shava, "A
562 simple mathematical model of Ebola in Africa", *Journal of Biological Dynamics*, 11:1,
563 42-74,DOI: 10.1080/17513758.20161229817, 2017.

- 564 [12] N. T. J. Bailey, and others. The mathematical theory of infectious diseases and its
565 applications, Charles Griffin & Company Ltd, 5a Crendon Street, High Wycombe, Bucks
566 HP13 6LE., 1975.
- 567 [13] R. M. Anderson. The population dynamics of infectious diseases: theory and applications,
568 Springer, 2013.
- 569 [14] H. R. Thieme. Convergence results and a Poincare-Bendison trichotomy for asymptotical
570 autonomous differential equations. *J. Math. Biol.* 30, 755-763, 1992.
- 571 [15] W. Wang and X-Q Zhao. Threshold dynamics for compartment epidemic models in
572 periodic environments. *Journal of Dynamics and Differential Equations*, 20:699-717, 2008.
- 573 [16] S. F. Dowel. Seasonal Variation in Host Susceptibility and Cycles of Certain Infectious
574 Diseases. *Emerging Infectious Diseases* 7: 369-374, 2001.
- 575 [17] Shuai, Z, Heesterbeek, J.A.P., van den Driessche, P. Extending the type reproduction
576 number to infectious disease control targeting contacts between types, *J. Math. Biol.* 67
577 (5)1067-1082, 2013.
- 578 [18] P. Van den Driessche and J. Watmough. Reproduction number and subthresh-
579 old endemic equilibria for compartment models of disease transmission. *Mathematical*
580 *Biosciences*, 180:29-48, 2002.
- 581 [19] M. Saeedian, and M. Khalighi, and N. Azimi-Tafreshi and G.R. Jafari, and M. Aus-
582 loos. Memory effects on epidemic evolution: The susceptible-infected-recovered epidemic
583 model, *Physical Review E*, Vol. 95, no. 2, pp. 022409, 2017.
- 584 [20] N. Hamdan, and A. Kilicman. Analysis of the fractional order dengue transmission model:
585 a case study in Malaysia, *Springer*, Vol. no.1, pp. 1-13, 2019.
- 586 [21] A. Mouaouine, and A. Boukhouima, and K. Hattaf, and N. Yousfi. A fractional order
587 SIR epidemic model with nonlinear incidence rate, *Springer*, pp. 1-9, 2018.
- 588 [22] J-G. Liu, X-J. Yang, Y-Y. Feng, L-L. Geng. Fundamental results to the weighted Caputo-
589 type differential operator. *Applied Mathematics Letters* 121, 107421, 2021.
- 590 [23] F.A. Rihan, and Q.M. Al-Mdallal, and H.J. AlSakaji, and A. Hashish. A fractional-order
591 epidemic model with time-delay and nonlinear incidence rate, *Elsevier*, Vol. 126, pp.
592 97-105, 2019.

- 593 [24] Vargas-De-Leó n., Volterra-type Lyapunov functions for fractional-order epidemic sys-
594 tems. *Commun, Nonlinear Sci. Numer. Simul.* **24**, 7585, 2015.
- 595 [25] M. Helikumi, M. Kgosimore, D. Kuznetsov, and S. Mushayabasa. A fractional-order Try-
596 panosoma brucei rhodesiense model with vector saturation and temperature dependent
597 parameters, Springer, no. 1, pp. 1-23, 2020.
- 598 [26] I. Area, H. Batarfi, J. Losada, J. J. Nieto, W. Shammakh , & A. Torres . ”On a fractional
599 order Ebola epidemic model”, *Advances in Difference Equations*, 2015(1), 1-12, 2015.
- 600 [27] M. Farman, A. Akgül, T. Abdeljawad, and P. A. Naik, and N. Bukhari, and A. Ahmad.
601 Modeling and analysis of fractional order Ebola virus model with Mittag-Leffler kernel,
602 Elsevier, Vol.61, no.3,pp. 2061-2073, 2022.
- 603 [28] M. A. Dokuyucu, and H. Dutta. A fractional order model for Ebola Virus with the new
604 Caputo fractional derivative without singular kernel, Elsevier, Vol. 134, pp. 109717, 2020.
- 605 [29] A. Raza, M. Farman, A. Akgül, M. S. Iqbal, and A. Ahmad. Simulation and numerical so-
606 lution of fractional order Ebola virus model with novel technique, *AIMS Bioengineering*,
607 Vol. 7, no. 4, pp. 194-207, 2020.
- 608 [30] H. Singh, ”Analysis for fractional dynamics of Ebola virus model”, *Chaos, Solitons &*
609 *Fractals*, 138, 109992, 2020.
- 610 [31] W. Pan, T. Li, and S. Ali. A fractional order epidemic model for the simulation of
611 outbreaks of Ebola, Springer, pp. 1-21, 2021.
- 612 [32] H. L. Li, L. Zhang, C. Hu, Y. L. Jiang, Z. Teng. Dynamical analysis of a fractional-order
613 predator-prey model incorporating a prey refuge. *Journal of Applied Mathematics and*
614 *Computing*, 54(1-2), 435-449, 2017.
- 615 [33] L.C. de Barros, M.M. Lopes, F. Santo Pedro, E. Esmi, J.P.C. dos Santos, and D.E.
616 Snchez. The memory effect on fractional calculus: an application in the spread of COVID-
617 19. *Computational and Applied Mathematics*, 40(3), pp.1-21, 2021.
- 618 [34] J. Huo, H. Zhao, L. Zhu . The effect of vaccines on backward bifurcation in a fractional
619 order HIV model. *Nonlinear Analysis: Real World Applications*, 26, 289-305, 2015.

- 620 [35] P. A. Naik, J. Zu, K. M. Owolabi. Global dynamics of a fractional order model for the
621 transmission of HIV epidemic with optimal control. *Chaos, Solitons & Fractals*, 138,
622 109826, 2020.
- 623 [36] K. M. Owolabi. Behavioural study of symbiosis dynamics via the Caputo and Atangan-
624 aBaleanu fractional derivatives. *Chaos, Solitons & Fractals*, 122, 89-101, 2019.
- 625 [37] K. M. Owolabi, A. Atangana. Mathematical analysis and computational experiments for
626 an epidemic system with nonlocal and nonsingular derivative. *Chaos, Solitons & Fractals*,
627 126, 41-49, 2019.
- 628 [38] Z. U. A. Zafar, K. Rehan, M. Mushtaq. HIV/AIDS epidemic fractional-order model.
629 *Journal of Difference Equations and applications*, 23(7), 1298-1315, 2017.
- 630 [39] K. Muhammad Altaf, & A. Atangana, "Dynamics of Ebola disease in the framework of
631 different fractional derivatives", *Entropy*, 21(3), 303, 2019.
- 632 [40] Z. Juan and M. Zhien. Global dynamics of an seir epidemic model with saturating contact
633 rate, *Mathematical Biosciences Journal*; 185,15-32, 2003.
- 634 [41] F. Nielsen Carie, S. Kidd, A.R. Sillah, E. Davis, J. Mermin, H. Kilmarx Peter, "Improving
635 burial practices and cemetery management during an Ebola virus disease epidemic-Sierra
636 Leone, 2014", *MMWR.*, 64(1):20, 2015.
- 637 [42] H.W. Berhe, S. Qureshi, and A. A. Shaikh. "Deterministic modeling of dysentery diar-
638 rhea epidemic under fractional Caputo differential operator via real statistical analysis",
639 *Chaos,Solitons & Fractals*, 131, p.109536, 2020.
- 640 [43] B. S. Alkahtani. Atangana-Batogna numerical scheme applied on a linear and non-linear
641 fractional differential equation, *The European Physical Journal Plus*, vol. 133, no. 3, pp.
642 110, 2018.
- 643 [44] J. Huo, H. Zhao, and L. Zhu. The effect of vaccines on backward bifurcation in a fractional
644 order HIV model, *Nonlinear Analysis: Real World Applications*, vol. 26, pp. 289305, 2015.
- 645 [45] H. Delavari, D. Baleanu, J. Sadati. "Stability analysis of Caputo fractional-order", *Non-*
646 *linear systems revisited, Nonlinear Dyn.*, **67**, 2433-2439, 2012.

- 647 [46] F.B. Aguston, M.I. Teboh-Wwaungkem, and A.B. Gumel, "Mathematical assessment of
648 the effect of traditional beliefs and customs on the transmission dynamics of the 2014
649 Ebola outbreak", *BMC MED.*, 13, p.96, 2015.
- 650 [47] B. Ivorra, D. Ngom and A.M. Ramos, Be-CodiS, "A mathematical model to predict
651 the risk of human diseases spread between countries-validation and application to the
652 2014-2015 ebola virus disease epidemic", *Bull. Math. Bio.* 77, pp 1668-1704, 2015.
- 653 [48] Li C, Zeng F (2013) The finite difference methods for fractional ordi-
654 nary differential equations. *Numer Funct Anal Optim* 34: 149-179. [http-
655 s://doi.org/10.1080/01630563.2012.706673](http://doi.org/10.1080/01630563.2012.706673)
- 656 [49] Liang S, Wu R, Chen L (2015) Laplace transform of fractional order differential equations.
657 *Electron J Differ Equ* 139: 2015. <http://ejde.math.txstate.edu>
- 658 [50] Kexue L, Jigen P (2011) Laplace transform and fractional differential equations. *Appl*
659 *Math Lett* 24: 2019-2023. <https://doi.org/10.1016/j.aml.2011.05.035>
- 660 [51] Podlubny I (1999) Fractional Differential Equations: An Introduction to Fractional
661 Derivatives, Fractional Differential Equations, to Methods of their Solution and some of
662 their Applications *Math Sci Eng* 7: 1-340. [https://doi.org/10.1016/s0076-5392\(99\)x8001-
663 5](https://doi.org/10.1016/s0076-5392(99)x8001-5)
- 664 [52] Chen M and Wu R, Dynamics of a depletion-type Gierer-Meinhardt model with
665 Langmuir- Hinshelwood reaction scheme. *Discrete and Continuous Dynamical Systems*
666 *Series B* 27(4) (2022) 22752312.
- 667 [53] Khalil, H. K., *Nonlinear Systems (Third edition)*, Prentice Hall, Englewood Cliffs, NJ,
668 2002.
- 669 [54] K. Diethelm, *The Analysis of Fractional Differential Equations: An Application-Oriented*
670 *Exposition Using Differential Operators of Caputo Type*, Springer Science & Business
671 Media, 2020.
- 672 [55] G. Chowell, N.W. Hengartner, C. Castillo-Chavez, P. W. Fenimore, and J.M. Hyman,
673 "The basic reproductive number of Ebola and the effects of public health measures: The
674 cases of Congo and Uganda", *J. Theo. Biol.*, 229, pp. 119-126, 2014.

- 675 [56] D. Fisman, E. Khoo, and A. Tuite, "Early epidemic dynamics of the the West
676 African 2014 Ebola outbreak: Estimates derived with a simple two Parameter mod-
677 el", *PLOS Curr. outbreaks*, sep 8. Edition 1 doi; 10.1371/ currents. outbreaks.
678 89cod3783f36958d96ebbae97348d571, 2014.
- 679 [57] J. Legrand, R.F. Grais, P.Y. Boelle, A.J. Valleron, and A. Flahault, "Understanding thd
680 dynamics of Ebola epidemics", *Epidemiol. Infect.*, 135, pp. 610-621, 2007.
- 681 [58] S. Towers, O. Patterson-Lomba, and C. Castillo-Chavez, "Temporal variations in the
682 reproduction number of the 2014 outbreaks", *PLOS Curr. outbreaks*, September 18,
683 2014.
- 684 [59] K. Bibby, L.W. Casson, E. Stachler, and C.N. Haas, "Ebola virus persistence in the
685 environment state of the knowledge and research needs", *Envoron. Sci. Technol. Lett.*
686 *2.*, pp. 2-6, 2015.
- 687 [60] T.J. Piercy, S. J. Smither, J. A. Steward, L. Eastaugh, and M.S. Lever, "The Survival
688 of filoviruses in liquids, on solid substrate and in a dynamic aerosol", *J. App. Microbio.*,
689 109(5), pp. 1531-1539, 2010.
- 690 [61] F.O Fasina, A. Shitu, D. Lazarus, O. Tomori, L. Simonsen, C. Viboud, and G.
691 Chowell, "Transmission dynamics and control of Ebola virus disease outbreak in
692 Nigeria, July to September 2014", *Euro Surviell.*, 19 (40): pii 20920. Available at:
693 <http://www.eurosurveillance.org/ViewArticle.aspx?ArticleId=20920>, 2014.
- 694 [62] D. Ndanguza, J.M. Tchuenche, and H. Haario, "Statistical data analysis of the 1995
695 outbreak in the Democratic Republic of Congo", *Afrika Mat.*, 24, pp. 55-68, 2013.
- 696 [63] L. Arriola, and Hyman, J., "Forward and adjoint sensitivity analysis with applications
697 in dynamical systems", *Lecture Notes in Linear Algebra and Optimization*, 2005.

698 **Appendix A: Mathematical concepts of fractional order**

699 Consider the following differential equation of any dynamical system:

$$700 \quad \frac{df(t)}{dt} = \beta f(t) \quad (30)$$

701 where β is any constant or parameter. In order to capture the influence of memory effects, we
 702 rewrite the differential equation (30) in terms of dependent integral as follows:

$$703 \quad \frac{df(t)}{dt} = \beta \int_{t_0}^t k(t - \xi) f(\xi) d\xi \quad (31)$$

704 In this case, $k(t - \xi)$ plays the role of the time dependent kernel and is equivalent to a delta
 705 $\delta(t - \xi)$ in a classical Markov process. This type of kernel provides the existence of important
 706 features which exist in real problems. Now let us consider the following power-law correlation
 707 function for $k(t - \xi)$:

$$708 \quad k(t - \xi) = \frac{1}{\Gamma(\alpha - 1)} (t - \xi)^{\alpha - 2} \quad (32)$$

709 where $\Gamma(\alpha)$ denotes the Gamma function and $0 < \alpha \leq 1$. In this case, the choice of coefficient
 710 $\Gamma(\alpha - 2)$ and the exponent $\alpha - 1$ allow to write the differential equation (30) to the form of
 711 fractional order derivative in Caputo sense. Substituting this kernel in (30) the right hand side
 712 of function leads to the fractional integral of order $(\alpha - 1)$ on the interval $[b, t]$, denoted by
 713 ${}_b D_{t_0}^{-(\alpha - 1)}$. Applying a fractional Caputo derivative of order $(\alpha - 1)$ in (30) and using the fact
 714 that both Caputo fractional derivative and fractional integral are inverse operators, one gets
 715 the following fractional differential equation:

$$716 \quad D_{t_0}^\alpha f(t) = \beta^\alpha f(t) dt \quad (33)$$

717 where $D_{t_0}^\alpha f(t)$ denotes the Caputo fractional derivative of order $\alpha \in (0, 1)$, defined for an
 718 arbitrary function $f(t)$ as:

$$719 \quad D_{t_0}^\alpha f(t) = \frac{1}{\Gamma(1 - \alpha)} \int_0^t \frac{\dot{f}(\xi)}{(t - \xi)^\alpha} d\xi. \quad (34)$$

720 Thus, the function (34) defines the fractional order derivatives in Caputo sense.

721 *Remarks* : Note that, In order to avoid flaws regarding the time dimension, we introduce the α
 722 in parameter β (right-hand side) of the differential equation (33) so that the dimension of the
 723 parameter β become $(time)^{-\alpha}$ which agree with the left-hand side of the differential equation.

724 **Definition 3.** For the differential equation described in (30)

725 (i) The trivial solution is said to be stable if, for every $t_0 \in \mathbb{R}$ and every $\epsilon > 0$, there exists
 726 $\delta = \delta(t_0, \epsilon)$ such that $\|x(t_0)\| < \delta \rightarrow \|x(t)\| < \epsilon$ for all $t > t_0$.

727 (ii) The trivial solution is said to be symptomatically stable if it is stable and, for any $t_0 \in \mathbb{R}$
 728 and any $\epsilon > 0$, there exists $\delta_a = \delta_a(t_0, \epsilon) > 0$ such that $\|x(t)\| < \delta_a \rightarrow \lim_{t \rightarrow \infty} \|x(t)\| = 0$

729 (iii) The trivial solution is said to be uniformly stable if it is stable and $\delta = \delta(\epsilon) > 0$ can be
 730 chosen independently of t_0 .

731 (iv) The trivial solution is uniformly asymptotically stable if it is uniformly stable and there
 732 exists δ_a independently of t_0 , such that if $\|x(t)\| < \delta_a$, then $\lim_{t \rightarrow \infty} \|x(t)\| = 0$.

733 (iii) The trivial solution is said to be uniformly stable if it is stable and $\delta = \delta(\epsilon) > 0$ can be
 734 chosen independently of t_0 .

735 (v) The trivial solution is globally asymptotically stable if it is asymptotically stable and
 736 δ_a can be any arbitrarily large finite number.

737 Appendix B: Non-negativity and boundedness of model solutions

738 In this section, we present the existence, uniqueness, positivity and boundedness of the solu-
 739 tions of model (2). We commence our discussion by demonstrating existence and uniqueness
 740 of solutions. Our approach is based on the fixed-point theory. Let \mathcal{B} be a Banach space of
 741 real-valued continuous functions defined on an interval \mathcal{I} with the associated norm:

$$742 \quad \|S, E, I, R, D, P\| = \|S\| + \|E\| + \|I\| + \|R\| + \|D\| + \|P\| \quad (35)$$

743 where $\|S\| = \sup\{|S(t)| : t \in \mathcal{I}\}$, $\|E\| = \sup\{|E(t)| : t \in \mathcal{I}\}$, $\|I\| = \sup\{|I(t)| : t \in \mathcal{I}\}$,
 744 $\|R\| = \sup\{|R(t)| : t \in \mathcal{I}\}$, $\|D\| = \sup\{|D(t)| : t \in \mathcal{I}\}$, $\|P\| = \sup\{|P(t)| : t \in \mathcal{I}\}$, and
 745 $\mathcal{B} = \mathcal{E}(\mathcal{I}) \times \mathcal{E}(\mathcal{I}) \times \mathcal{E}(\mathcal{I}) \times \mathcal{E}(\mathcal{I}) \times \mathcal{E}(\mathcal{I}) \times \mathcal{E}(\mathcal{I}) \times \mathcal{E}(\mathcal{I})$, with $\mathcal{E}(\mathcal{I})$ denoting the Banach space
 746 of real-valued continuous functions on \mathcal{I} and the associated sup norm. The model system (2)
 747 can be rewritten in the the following form:

$$748 \quad \left. \begin{aligned} D_{t_0}^\alpha S(t) &= G_1(t, S), \\ D_{t_0}^\alpha E(t) &= G_2(t, E), \\ D_{t_0}^\alpha I(t) &= G_3(t, I), \\ D_{t_0}^\alpha R(t) &= G_4(t, R), \\ D_{t_0}^\alpha D(t) &= G_5(t, D), \\ D_{t_0}^\alpha P(t) &= G_6(t, P), \end{aligned} \right\} \quad (36)$$

749 By applying the Caputo fractional integral operator, system (36), reduces to the following
 750 integral equation of Volterra type with Caputo fractional integral of order $0 < \alpha < 1$,

$$\left. \begin{aligned}
 S(t) - S(0) &= \frac{1}{\Gamma(\alpha)} \int_0^t (t - \chi)^{\alpha-1} G_1(\chi, S) d\chi, \\
 E(t) - E(0) &= \frac{1}{\Gamma(\alpha)} \int_0^t (t - \chi)^{\alpha-1} G_2(\chi, E) d\chi, \\
 I(t) - I(0) &= \frac{1}{\Gamma(\alpha)} \int_0^t (t - \chi)^{\alpha-1} G_3(\chi, I) d\chi, \\
 R(t) - R(0) &= \frac{1}{\Gamma(\alpha)} \int_0^t (t - \chi)^{\alpha-1} G_4(\chi, I) d\chi, \\
 D(t) - D(0) &= \frac{1}{\Gamma(\alpha)} \int_0^t (t - \chi)^{\alpha-1} G_5(\chi, D) d\chi, \\
 P(t) - P(0) &= \frac{1}{\Gamma(\alpha)} \int_0^t (t - \chi)^{\alpha-1} G_6(\chi, P) d\chi,
 \end{aligned} \right\} \quad (37)$$

752 What follows, we prove that the kernels G_i , $i = 1, 2, 3, 4, 5, 6$ fulfill the Lipschitz condition and
 753 contraction under some assumptions. In the following theorem, we have demonstrated for G_1
 754 and one can easily verify for the remainder.

755 **Theorem 5.1.** *Let us consider the following inequality*

$$0 \leq (\beta_1 k_1 + \beta_2 k_2 + \lambda k_3 + \mu + \psi) < 1.$$

757 *The kernel G_1 satisfies the Lipschitz condition as well as contraction if the above inequality is*
 758 *satisfied.*

759 *Proof.* For S and S_1 we proceed as below.

$$\begin{aligned}
 \|G_1(t, S) - G_1(t, S_1)\| &= \| -((\beta_1 k_1 + \beta_2 k_2 + \lambda k_3 + \mu + \psi))(S(t) - S_1(t)) \\
 &= (\mu + \psi) \|S - S_1\| + \beta_1 I + \beta_2 D + \lambda P \| (S - S_1) \|. \quad (38)
 \end{aligned}$$

761 Since $I(t)$, $D(t)$ and $P(t)$ are bounded functions, i.e, $\|I\| \leq k_1$, $\|D\| \leq k_2$ and $\|P\| \leq k_3$, by
 762 the property of norm functions, the above inequality (38) can be written as

$$\|G_1(t, S) - G_1(t, S_1)\| \leq \eta_1 \|S(t) - S_1(t)\|, \quad (39)$$

764 where $\eta_1 = \beta_1 k_1 + \beta_2 k_2 + \lambda k_3 + \mu + \psi$. Hence for G_1 the Lipschitz condition is obtained and
 765 if an additionally $0 \leq \beta_1 k_1 + \beta_2 k_2 + \lambda k_3 + \mu + \psi < 1$, we obtain a contraction. The Lipschitz
 766 condition for the other kernels are

$$\left. \begin{aligned}
 \|G_2(t, E) - G_2(t, E_1)\| &\leq \eta_2 \|E(t) - E_1(t)\|, \\
 \|G_3(t, I) - G_3(t, I_1)\| &\leq \eta_3 \|I(t) - I_1(t)\|, \\
 \|G_4(t, R) - G_4(t, R_1)\| &\leq \eta_4 \|R(t) - R_1(t)\|, \\
 \|G_5(t, D) - G_5(t, D_1)\| &\leq \eta_5 \|D(t) - D_1(t)\|, \\
 \|G_6(t, P) - G_6(t, P_1)\| &\leq \eta_6 \|P(t) - P_1(t)\|,
 \end{aligned} \right\} \quad (40)$$

768 □

769 Recursively, the expression in (37) can be written as

$$\left. \begin{aligned}
 S_n(t) - S(0) &= \frac{1}{\Gamma(\alpha)} \int_0^t (t - \chi)^{\alpha-1} G_1(\chi, S_{n-1}) d\chi, \\
 E_n(t) - E(0) &= \frac{1}{\Gamma(\alpha)} \int_0^t (t - \chi)^{\alpha-1} G_2(\chi, E_{n-1}) d\chi, \\
 I_n(t) - I(0) &= \frac{1}{\Gamma(\alpha)} \int_0^t (t - \chi)^{\alpha-1} G_3(\chi, I_{n-1}) d\chi, \\
 R_n(t) - R(0) &= \frac{1}{\Gamma(\alpha)} \int_0^t (t - \chi)^{\alpha-1} G_4(\chi, R_{n-1}) d\chi, \\
 D_n(t) - D(0) &= \frac{1}{\Gamma(\alpha)} \int_0^t (t - \chi)^{\alpha-1} G_5(\chi, D_{n-1}) d\chi, \\
 P_n(t) - P(0) &= \frac{1}{\Gamma(\alpha)} \int_0^t (t - \chi)^{\alpha-1} G_6(\chi, P_{n-1}) d\chi,
 \end{aligned} \right\} \quad (41)$$

771 The difference between successive terms of system (36) in recursive form is given below:

$$\left. \begin{aligned}
 \phi_{1n} &= S_n(t) - S_{n-1}(t) \\
 &= \frac{1}{\Gamma(\alpha)} \int_0^t (t - \chi)^{\alpha-1} (G_1(\chi, S_{n-1}) - G_1(\chi, S_{n-2})) d\chi, \\
 \phi_{2n} &= E_n(t) - E_{n-1}(t) \\
 &= \frac{1}{\Gamma(\alpha)} \int_0^t (t - \chi)^{\alpha-1} (G_2(\chi, E_{n-1}) - G_2(\chi, E_{n-2})) d\chi, \\
 \phi_{3n} &= I_n(t) - I_{n-1}(t) \\
 &= \frac{1}{\Gamma(\alpha)} \int_0^t (t - \chi)^{\alpha-1} (G_3(\chi, I_{n-1}) - G_3(\chi, I_{n-2})) d\chi, \\
 \phi_{4n} &= R_n(t) - R_{n-1}(t) \\
 &= \frac{1}{\Gamma(\alpha)} \int_0^t (t - \chi)^{\alpha-1} (G_4(\chi, R_{n-1}) - G_4(\chi, R_{n-2})) d\chi, \\
 \phi_{5n} &= D_n(t) - D_{n-1}(t) \\
 &= \frac{1}{\Gamma(\alpha)} \int_0^t (t - \chi)^{\alpha-1} (G_5(\chi, D_{n-1}) - G_5(\chi, D_{n-2})) d\chi, \\
 \phi_{6n} &= P_n(t) - P_{n-1}(t) \\
 &= \frac{1}{\Gamma(\alpha)} \int_0^t (t - \chi)^{\alpha-1} (G_6(\chi, P_{n-1}) - G_6(\chi, P_{n-2})) d\chi,
 \end{aligned} \right\} \quad (42)$$

773 with the initial conditions $S_0(t) = S(0)$, $E_0(t) = E(0)$, $I_0(t) = I$, $R_0(t) = R(0)$, $D_0(t) = D(0)$
 774 and $P_0(t) = P_0$. Taking the norm of the first equation of (42), we obtain

$$\begin{aligned}
 \|\phi_{1n}(t)\| &= \|S_n(t) - S_{n-1}(t)\| \\
 &= \left\| \frac{1}{\Gamma(\alpha)} \int_0^t (t - \chi)^{\alpha-1} (G_1(\chi, S_{n-1}) - G_1(\chi, S_{n-2})) d\chi \right\| \\
 &\leq \frac{1}{\Gamma(\alpha)} \int_0^t (t - \chi)^{\alpha-1} \|G_1(\chi, S_{n-1}) - G_1(\chi, S_{n-2})\| d\chi.
 \end{aligned} \quad (43)$$

776 Applying the Lipschitz condition (39) one gets

$$\|\phi_{1n}(t)\| \leq \frac{1}{\Gamma(\alpha)} \eta_1 \int_0^t (t - \chi)^{\alpha-1} \|S_{n-1} - S_{n-2}\| d\chi. \quad (44)$$

778 Thus, we have

$$\|\phi_{1n}(t)\| \leq \frac{1}{\Gamma(\alpha)} \eta_1 \int_0^t (t - \chi)^{\alpha-1} \|\phi_{1n}(t)\| d\chi. \quad (45)$$

780 Similarly, for the remainder of the equations in system (2) we have

$$\left. \begin{aligned}
 \|\phi_{2n}(t)\| &\leq \frac{1}{\Gamma(\alpha)}\eta_2 \int_0^t (t-\chi)^{\alpha-1} \|\phi_{2n}(t)\| d\chi, \\
 \|\phi_{3n}(t)\| &\leq \frac{1}{\Gamma(\alpha)}\eta_3 \int_0^t (t-\chi)^{\alpha-1} \|\phi_{3n}(t)\| d\chi, \\
 \|\phi_{4n}(t)\| &\leq \frac{1}{\Gamma(\alpha)}\eta_4 \int_0^t (t-\chi)^{\alpha-1} \|\phi_{4n}(t)\| d\chi, \\
 \|\phi_{5n}(t)\| &\leq \frac{1}{\Gamma(\alpha)}\eta_5 \int_0^t (t-\chi)^{\alpha-1} \|\phi_{5n}(t)\| d\chi, \\
 \|\phi_{6n}(t)\| &\leq \frac{1}{\Gamma(\alpha)}\eta_6 \int_0^t (t-\chi)^{\alpha-1} \|\phi_{6n}(t)\| d\chi,
 \end{aligned} \right\} \quad (46)$$

782 From (46) one can write

$$\left. \begin{aligned}
 S_n(t) &= \sum_{i=1}^n \phi_{1i}(t), & E_n(t) &= \sum_{i=1}^n \phi_{2i}(t), & I_n(t) &= \sum_{i=1}^n \phi_{3i}(t), \\
 R_n(t) &= \sum_{i=1}^n \phi_{4i}(t), & D_n(t) &= \sum_{i=1}^n \phi_{5i}(t), & P_n(t) &= \sum_{i=1}^n \phi_{6i}(t),
 \end{aligned} \right\} \quad (47)$$

784 Now, we claim the following result which guaranteed the uniqueness of solution of model (2).

785 **Theorem 5.2.** *The proposed fractional epidemic model (2) has a unique solution for $t \in [0, T]$*
 786 *if the following inequality holds*

$$\frac{1}{\Gamma(\alpha)} b^\alpha \eta_i < 1, \quad i = 1, 2, \dots, 7. \quad (48)$$

788 *Proof.* Earlier we have shown that the kernels conditions given in Eqs. (39) and (40) holds.

789 Thus by considering the Eqs. (46) and (48), and by applying the recursive technique we

790 obtained the succeeding results as below:

$$\left. \begin{aligned}
 \|\phi_{1n}(t)\| &\leq \|S_0(t)\| \left[\frac{1}{\Gamma(\alpha)} b^\alpha \eta_1 \right]^n, & \|\phi_{2n}(t)\| &\leq \|E_0(t)\| \left[\frac{1}{\Gamma(\alpha)} b^\alpha \eta_2 \right]^n, \\
 \|\phi_{3n}(t)\| &\leq \|I_0(t)\| \left[\frac{1}{\Gamma(\alpha)} b^\alpha \eta_3 \right]^n, \\
 \|\phi_{4n}(t)\| &\leq \|R_0(t)\| \left[\frac{1}{\Gamma(\alpha)} b^\alpha \eta_4 \right]^n, & \|\phi_{5n}(t)\| &\leq \|D_0(t)\| \left[\frac{1}{\Gamma(\alpha)} b^\alpha \eta_5 \right]^n, \\
 \|\phi_{6n}(t)\| &\leq \|P_0(t)\| \left[\frac{1}{\Gamma(\alpha)} b^\alpha \eta_6 \right]^n,
 \end{aligned} \right\} \quad (49)$$

792 Therefore, the above mentioned sequences exist and satisfy $\|\phi_{1n}(t)\| \rightarrow 0$, $\|\phi_{2n}(t)\| \rightarrow 0$,

793 $\|\phi_{3n}(t)\| \rightarrow 0$, $\|\phi_{4n}(t)\| \rightarrow 0$, $\|\phi_{5n}(t)\| \rightarrow 0$, and $\|\phi_{6n}(t)\| \rightarrow 0$. Furthermore, from Eq. (49) and

794 employing the triangle inequality for any k , we one gets

$$\left. \begin{aligned}
 \|S_{n+k}(t) - S_n(t)\| &\leq \sum_{j=n+1}^{n+k} T_1^j = \frac{T_1^{n+1} - T_1^{n+k+1}}{1 - T_1}, \\
 \|E_{n+k}(t) - E_n(t)\| &\leq \sum_{j=n+1}^{n+k} T_2^j = \frac{T_2^{n+1} - T_2^{n+k+1}}{1 - T_2}, \\
 \|I_{n+k}(t) - I_n(t)\| &\leq \sum_{j=n+1}^{n+k} T_3^j = \frac{T_3^{n+1} - T_3^{n+k+1}}{1 - T_3}, \\
 \|R_{n+k}(t) - R_n(t)\| &\leq \sum_{j=n+1}^{n+k} T_4^j = \frac{T_4^{n+1} - T_4^{n+k+1}}{1 - T_4}, \\
 \|D_{n+k}(t) - D_n(t)\| &\leq \sum_{j=n+1}^{n+k} T_5^j = \frac{T_5^{n+1} - T_5^{n+k+1}}{1 - T_5}, \\
 \|P_{n+k}(t) - P_n(t)\| &\leq \sum_{j=n+1}^{n+k} T_6^j = \frac{T_6^{n+1} - T_6^{n+k+1}}{1 - T_6},
 \end{aligned} \right\} \tag{50}$$

796 where $T_i = \frac{1}{\Gamma(q)} b^q \eta_i < 1$ by hypothesis. Therefore, S_n, E_n, I_n, R_n, D_n and P_n are regarded as
 797 Cauchy sequences in the Banach space $B(J)$. Hence they are uniformly convergent as described
 798 in [48]. Applying the limit theory on Eq. (41) when $n \rightarrow \infty$ affirms that the limit of these
 799 sequences is the unique solution of system (2). Ultimately, the existence of a unique solution
 800 for system (2) has been achieved. \square

801 We now demonstrate the positivity of solutions for all $t \geq 0$. To prove positivity and bounded-
 802 ness of solutions, we need the following Generalized Mean Value Theorem in [?] and corollary.

803 **Lemma 1.** *Suppose that $f(x) \in C[a, b]$ and $D_{t_0}^\alpha f(x) \in C[a, b]$, for $0 < \alpha \leq 1$, then we have*

$$804 \quad f(x) = f(a) + \frac{1}{\Gamma(\alpha)} (D_{t_0}^\alpha f)(\xi) (x - a)^\alpha \tag{51}$$

805 *with $a \leq \xi x, \forall x \in (a, b]$ and $\Gamma(\cdot)$ is the gamma function.*

806 **Corollary 1.** *Suppose that $f(x) \in C[a, b]$ and $D_{t_0}^\alpha f(x) \in C(a, b]$, for $0 < \alpha \leq 1$. If $D_{t_0}^\alpha f(x) \geq 0$,
 807 $\forall x \in (a, b)$, then $f(x)$ is non-decreasing for each $x \in [a, b]$. If $D_{t_0}^\alpha f(x) \leq 0, \forall x \in (a, b)$, then
 808 $f(x)$ is non-increasing for each $x \in [a, b]$.*

809 We now prove that the non-negative orthant \mathbb{R}_+^6 is positively invariant region. To do this,
 810 we need to show that on each hyperplane bounding the non-negative orthant, the vector field

811 points to \mathbb{R}_+^6 . From model (2), one gets:

$$812 \quad D_{t_0}^\alpha S(t)|_{S=0} = \Lambda^\alpha \geq 0, \quad (52)$$

$$813 \quad D_{t_0}^\alpha E(t)|_{E=0} = \psi^\alpha S(t) \geq 0, \quad (53)$$

$$814 \quad D_{t_0}^\alpha I(t)|_{I=0} = (\beta_1^\alpha I(t) + \beta_2^\alpha D(t) + \lambda^\alpha P(t))(S(t) + \gamma^\alpha E(t)) \geq 0, \quad (54)$$

$$815 \quad D_{t_0}^\alpha R(t)|_{R=0} = \sigma^\alpha I(t) \geq 0, \quad (55)$$

$$816 \quad D_{t_0}^\alpha D(t)|_{D=0} = (\mu^\alpha + \delta^\alpha)I(t) \geq 0, \quad (56)$$

$$817 \quad D_{t_0}^\alpha P(t)|_{P=0} = \rho^\alpha I(t) + \theta^\alpha D(t) \geq 0, \quad (57)$$

818 Thus, by Corollary 1, the solution of model (2) are always positive for $t \geq 0$. We now demon-
819 strate that all solutions of model (2) are bounded above for all $t \geq 0$. To do this, we need the
820 following Lemma 2 and Lemma 3.

821 **Lemma 2.** (see [49]). Let $\alpha > 0$, $n - 1 < \alpha < n - \mathbb{N}$. Suppose that $f(t), f'(t), \dots, f^{(n-1)}(t)$ are
822 continuous on $[t_0, \infty)$ and the exponential order and that $D_{t_0}^\alpha f(t)$ is piecewise continuous on
823 $[t_0, \infty)$. Then

$$824 \quad \mathcal{L}\{D_{t_0}^\alpha f(t)\} = s^\alpha \mathcal{F}(s) - \sum_{k=0}^{n-1} s^{\alpha-k-1} f^{(k)}(t_0) \quad (58)$$

825 where $\mathcal{F}(s) = \mathcal{L}\{f(t)\}$.

826 **Lemma 3.** (see [50]). Let \mathbb{C} be the complex plane. For any $\alpha > 0$ $\beta > 0$, and $A \in \mathbb{C}^{n \times n}$, we
827 have

$$828 \quad \mathcal{L}\{t^{\beta-1} E_{\alpha,\beta}(At^\alpha)\} = s^{\alpha-\beta} (s^\alpha - A)^{-1},$$

829 for $\mathcal{R}s > \|A\|^\frac{1}{\alpha}$, where $\mathcal{R}s$ represents the real part of the complex number s , and $E_{\alpha,\beta}$ is the
830 Mittag-Leffler function [51].

831 Since all solutions of model system (2) have been shown to be positively invariant and have a
832 lower bound zero (52)-(57), we now proceed to demonstrate that these solutions are bounded
833 above. By summing all equations of system (2) one gets:

$$834 \quad \begin{aligned} D_{t_0}^\alpha N(t) &= \Lambda^\alpha - \mu^\alpha N(t) - \epsilon^\alpha D(t) - (\tau^\alpha + \eta^\alpha)P(t) \\ &\leq \Lambda^\alpha - \mu^\alpha N(t). \end{aligned} \quad (59)$$

835 Taking the Laplace transform of (59) leads to:

$$836 \quad s^\alpha \mathcal{L}(N(t)) - s^{\alpha-1} N(0) \leq \frac{\Lambda^\alpha}{s} - \mu^\alpha \mathcal{L}(N(t)). \quad (60)$$

837 Combining like terms and arranging leads to

$$\begin{aligned}
 \mathcal{L}(N(t)) &\leq \Lambda^\alpha \frac{s^{-1}}{s^\alpha + \mu^\alpha} + N(0) \frac{s^{\alpha-1}}{s^\alpha + \mu^\alpha} \\
 &= \Lambda^\alpha \frac{s^{\alpha-(1+\alpha)}}{s^\alpha + \mu^\alpha} + N(0) \frac{s^{\alpha-1}}{s^\alpha + \mu^\alpha}.
 \end{aligned}
 \tag{61}$$

839 Applying the inverse Laplace transform leads to

$$\begin{aligned}
 N(t) &\leq \mathcal{L}^{-1} \left\{ \Lambda^\alpha \frac{s^{-1}}{s^\alpha + \mu^\alpha} + N(0) \frac{s^{\alpha-1}}{s^\alpha + \mu^\alpha} \right\} + \mathcal{L}^{-1} \left\{ N(0) \frac{s^{\alpha-1}}{s^\alpha + \mu^\alpha} \right\} \\
 &\leq \Lambda^\alpha t^\alpha E_{\alpha, \alpha+1}(-\mu t^\alpha) + N(0) E_{\alpha, 1}(-\mu t^\alpha) \\
 &\leq \frac{\Lambda^v}{\mu^\alpha} \mu^\alpha t^\alpha E_{\alpha, \alpha+1}(-\mu t^\alpha) + N(0) E_{\alpha, 1}(-\mu t^\alpha) \\
 &\leq \max \left\{ \frac{\Lambda^\alpha}{\mu^\alpha}, N(0) \right\} (\mu^\alpha t^\alpha E_{\alpha, \alpha+1}(-\mu t^\alpha) + E_{\alpha, 1}(-\mu t^\alpha)) \\
 &= \frac{C}{\Gamma(1)} = C,
 \end{aligned}
 \tag{62}$$

840 where $C = \max \left\{ \frac{\Lambda^\alpha}{\mu^\alpha}, N(0) \right\}$. Thus, $N(t)$ is bounded from above. This completes the proof of
 841
 842 Theorem (3.1).